Beyond Consensus: Embracing Heterogeneity in Neuroimaging Meta-Analysis

Gia H. Ngo[1], Simon B. Eickhoff[2,3], Peter T. Fox[4,5], R. Nathan Spreng[6], B.T. Thomas Yeo[1,7,8]

[1] Department of Electrical and Computer Engineering, ASTAR-NUS Clinical Imaging Research Centre, Singapore Institute for Neurotechnology and Memory Networks Program, National University of Singapore, Singapore [2]Institute for Systems Neuroscience, Medical Faculty, Heinrich-Heine University, Düsseldorf, Germany [3]Institute of Neuroscience and Medicine (INM-1, INM-7), Research Center Jülich, Jülich, Germany [4]Research Imaging Institute, University of Texas Health Science Center at San Antonio, San Antonio, TX, USA [5]South Texas Veterans Health Care System, San Antonio, TX, USA [6]Laboratory of Brain and Cognition, Montreal Neurological Institute, McGill University, Montreal, QC, Canada [7]Martinos Center for Biomedical Imaging, Massachusetts General Hospital, Charlestown, MA, USA [8]Centre for Cognitive Neuroscience, Duke-NUS Medical School, Singapore

Address correspondence to:

B.T. Thomas Yeo
ECE, ASTAR-NUS CIRC, SINAPSE & MNP
National University of Singapore
Email: thomas.yeo@nus.edu.sg

Abstract

Coordinate-based meta-analysis can provide important insights into mind-brain relationships. A popular meta-analytic approach is activation likelihood estimation (ALE), which identifies brain regions consistently activated across a selected set of experiments, such as within a functional domain or mental disorder. ALE can also be utilized in meta-analytic co-activation modeling (MACM) to identify brain regions consistently co-activated with a seed region. Therefore ALE aims to find consensus across experiments, treating heterogeneity across experiments as noise. However, heterogeneity within an ALE analysis of a functional domain might indicate the presence of functional sub-domains. Similarly, heterogeneity within a MACM analysis might indicate the involvement of a seed region in multiple co-activation patterns that are dependent on task contexts. Here we demonstrate the use of the author-topic model to automatically determine if heterogeneities within ALE-type meta-analyses can be robustly explained by a small number of latent patterns. In the first application, the author-topic modeling of experiments involving self-generated thought (N = 179) revealed two cognitive components fractionating the default network. In the second application, the author-topic model revealed that the inferior frontal junction (IFJ) participated in three co-activation patterns (N = 323), which are differentially expressed depending on cognitive demands of different tasks. Overall the results suggest that the author-topic model is a flexible tool for exploring heterogeneity in ALE-type meta-analyses that might arise from functional subdomains, mental disorder subtypes or task-dependent co-activation patterns. Code and data for this study are publicly available at GITHUB_LINK_TO_BE_ADDED.

Keywords:

theory of mind, autobiographical memory, executive function, inhibition, attentional control, mental disorder subtypes

Introduction

Magnetic resonance imaging (MRI) experiments of the human brain are often underpowered (Wager et al. 2009; Carp, 2012; Poline et al., 2012; Button et al., 2013; David et al. 2013). Because many neuroimaging studies report activation coordinates in common coordinate systems (e.g., MNI152), coordinate based meta-analysis provides an important framework (Turkeltaub et al. 2002; Chein et al. 2002; Wager et al. 2003; Eickhoff et al., 2009; Fox et al. 2014; Poldrack and Yarkoni, 2016) for analyzing underpowered studies across different experimental conditions and analysis piplines in order to reveal reliable trends (Smith et al., 2009; Shackman et al., 2011; Phillip et al., 2012) or null effects (Nickl-Jockschat 2015; Müller et al., 2017).

Large-scale coordinate-based meta-analyses might involve thousands of experiments across diverse experimental designs (Smith et al., 2009; Laird et al., 2011; Poldrack et al., 2011; Crossley et al., 2014; Yeo et al., 2015; Bertolero et al., 2015). The goal of these large-scale meta-analyses is to discover broad and general principles of brain organization and disorder. By contrast, the vast majority of meta-analyses involve smaller number of experiments, the goal of which is to generate consensus on specific functional domains (e.g., Binder et al. 2009), brain regions (e.g., Shackman et al., 2011) or disorders (e.g., Cortese et al., 2012).

A popular approach for these smaller-scale meta-analyses is activation likelihood estimation or ALE (Turkeltaub et al. 2002; Laird et al., 2005; Eickhoff et al. 2009, 2012; Turkeltaub et al. 2012). ALE identifies brain regions consistently activated across neuroimaging experiments within a functional domain (Rottschy et. al., 2012; Spaniol et al., 2009, Decety and Lamm, 2007, Costafreda et al., 2008, Beissner et al., 2013) or within a disease (e.g., Glahn et al., 2005; Minzenberg et al., 2009; Ragland et al., 2009; Fitzgerald et al., 2008; Delaveu et al., 2011; Kuhn and Gallinat, 2013; Di Martino et al., 2009; Phillip et al., 2012). ALE can also be utilized in meta-analytic connectivity modeling or MACM (Toro et al., 2008; Koski and Paus, 2010; Robinson et al., 2010; Eickhoff et al., 2010) to identify brain regions that consistently co-activate with a particular seed region. MACM has provided insights into functionally distinct sub-regions, such as those within lateral prefrontal cortex (Reid et al., 2016), insula (Cauda et al., 2012; Clos et al., 2014) and orbitofrontal cortex (Zald et al. 2014).

A key feature of ALE is that it seeks consensus across neuroimaging experiments. However, by treating heterogeneities across studies as noise, ALE

analysis of a functional domain might miss out on genuine biological heterogeneity indicative of functional sub-domains. Similarly, MACM of a seed region might miss out on heterogeneity indicative of the seed region involving in multiple co-activation patterns depending on task contexts. One way to address this issue is for meta-analyses to *manually* subdivide experiments into smaller domains based on specific hypotheses. For example, a recent ALE meta-analysis of working memory further divided the experiments into verbal versus non-verbal working memory tasks, as well as tasks involving object identity versus object locations (Rottschy et al., 2012).

In this work, we propose the use of the author-topic model to automatically make sense of heterogeneity within ALE-type meta-analyses. We have previously utilized the author-topic model (Figure 1; Yeo et al. 2015; Bertolero et al., 2015) to encode the intuitive notion that a behavioral task recruits multiple cognitive components, which are in turn supported by overlapping brain regions (Mesulam 1990; Poldrack 2006; Barrett and Satpute, 2013). While our previous work focused on

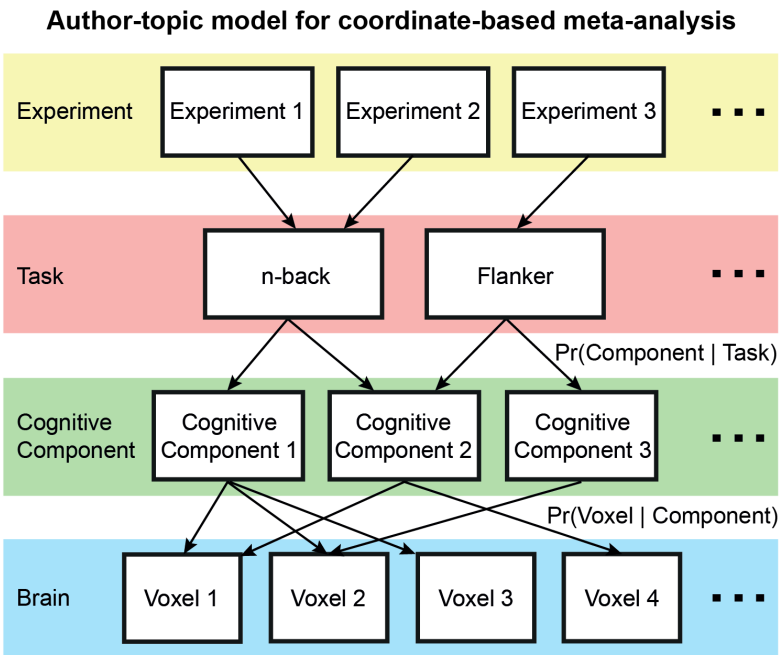

Figure 1. Author-topic model for coordinate-based meta-analysis (Yeo et al., 2015). Behavioral tasks recruit multiple cognitive components, which are in turn supported by overlapping brain regions. The model parameters are the probability that a task would recruit a cognitive component (Pr(component | task)) and the probability that a component would activate a brain voxel (Pr(voxel | component)).

large-scale meta-analysis across many functional domains (Yeo et al. 2015; Bertolero et al., 2015), the current study focuses on heterogeneity within a functional domain or co-activation heterogeneity of a seed region. These applications of the author-topic

model are made possible by the development of a novel inference algorithm for the author-topic model (Ngo et al., 2016) that is sufficiently robust for smaller-scale meta-analyses.

We demonstrate our approach with two applications. The first application focuses on the functional domain of self-generated thought. Self-generated thought often involves an associative and constructive processes that take place within an individual, and depends upon an internal representation to reconstruct or imagine a situation, understand a stimulus, or generate an answer to a question. The term "self-generated thought" serves to contrast with thoughts where the primary referent is based on immediate perceptual input (Andrews-Hanna et al., 2014). By virtue of being largely stimulus independent or task unrelated, self-generated thought has been linked with the functions of the default network (Buckner et al., 2008; Andrews-Hanna et al., 2014). The default network is a collection of brain regions with heightened activity during passive task states (Raichle et al., 2001; Buckner et al. 2008). Previous ALE meta-analyses have implicated the default network in many tasks involving self-generated thought, including theory of mind, episodic memory and moral cognition (Spreng et al. 2009; Binder et al. 2009; Mar et al., 2011; Sevinc and Spreng, 2014). However, some neuroimaging meta-analyses and empirical studies have suggested that the default network might be fractionated into sub-regions or sub-systems (Laird et al. 2009; Andrews-Hanna et al., 2010; Yeo et al. 2014; Andrews-Hanna et al., 2014). A functional fractionation of the default network has been proposed, wherein there is a dorsomedial prefrontal subsystem, more specialized for social cognition and narrative processing (Andrews-Hanna et al., 2014; Spreng & Andrews-Hanna, 2015). A second subsystem involves the medial temporal lobes, which play a specific role in mnemonic constructive processes (Andrews-Hanna et al., 2014; Christoff et al., 2016). However, the specific fractionation details differed across studies (Laird et al. 2009; Mayer et al. 2010; Andrews-Hanna et al., 2014; Humphreys et al., 2015), so the author-topic model might potentially clarify cognitive components subserving self-generated thought.

In the second application, the author-topic model was utilized to investigate the co-activation heterogeneity of the left inferior frontal junction (IFJ). The IFJ region was delineated in a previous study using MACM and co-activation based parcellation (Muhle-Karbe et al., 2015). In that study, the IFJ seed region was found to exhibit a "global" co-activation pattern distinctively different from neighboring

regions. However, the global co-activation pattern revealed by MACM might potentially comprise multiple co-activation patterns. Indeed, the IFJ has been implicated in many cognitive processes (Brass and Cramon, 2002; Brass et al. 2005; Derfuss et al. 2004, 2005; Asplund et al. 2010; Baldauf and Desimone, 2014; Chikazoe et al. 2009; Levy and Wagner, 2011; Zanto et al. 2010; Sneve et al. 2013, Kim et al. 2011; Yeo et al., 2015) and is also a key node of the multiple-demand system (Duncan et al., 2010; Fedorenko et al., 2010). In graph theoretic analysis of resting-state fMRI, the IFJ has been shown to be a connector hub (Bertolero et al., 2015) that coordinates information across modules. By adapting the author-topic model for co-activation analyses, we seek to determine if the IFJ is involved in multiple co-activation patterns that are dependent on task contexts.

Methods

Overview

We first review the author-topic model for coordinate-based meta-analysis (Yeo et al. 2015). The model was then utilized in two different applications. In the first application, we applied the author-topic model to discover cognitive components subserving self-generated thought. The model captures the premise that tasks involving self-generated thoughts recruit one or more cognitive components, supported by overlapping brain regions. In the second application, we estimated the co-activation patterns of the IFJ. The model is driven by the premise that the IFJ expresses one or more co-activation patterns; an experiment activating the IFJ can recruit one or more co-activation patterns.

Author-Topic Hierarchical Bayesian Model

The author-topic model was originally developed to discover topics from a corpus of text documents (Rosen-Zvi et al., 2010). The model represents each text document as an unordered collection of words written by a group of authors. Each author is associated with a probability distribution over topics, and each topic is associated with a probability distribution over a dictionary of words. Given a corpus of text documents, there are algorithms to estimate the distribution of topics associated with each author and the distribution of words associated with each topic. A topic is in some sense abstract, but is made concrete by its association with certain words and its association with certain authors. For example, if the author-topic model was applied to neuroimaging research articles, the algorithm might yield a topic associated with the author Stephen Smith and words like “fMRI”, “resting-state” and “ICA”. One might then interpret the topic posthoc as a “resting-state fMRI” research topic.

The author-topic model was applied to neuroimaging meta-analysis (Figure 1) by treating experimental contrasts in the BrainMap database (Fox and Lancaster, 2002) as text documents, 83 BrainMap task categories (e.g., n-back) as authors, cognitive components as topics, and activation foci as words in the documents (Yeo et al. 2015). Thus, the model encodes the premise that different behavioral tasks recruit multiple cognitive components, supported by overlapping brain regions.

Suppose a study utilizes one or more task categories, resulting in an experimental contrast yielding a collection of activation foci. Under the author-topic

model, each activation focus is assumed to be generated by first randomly selecting a task from the set of tasks utilized in the experiment. Given the task, a component is randomly chosen based on the probability of a task recruiting a component (Pr(component | task)). Given the component, the location of the activation focus is then randomly chosen based on the probability that the component would activate a voxel (Pr(voxel | component)). The entire collections of Pr(component | task) and Pr(voxel | component) are denoted as matrices θ and β, respectively. For example, the 2nd row and 3rd column of θ corresponds to Pr(3rd component | 2nd task) and the 4th row and 28th column of β corresponds to Pr(28th voxel | 4th component). Therefore each row of θ and β sums to 1. The formal mathematical definition of the model is provided in Appendix A1.

A key property of the author-topic model is that the ordering of words within a document is exchangeable. When applied to meta-analysis, the corresponding assumption is that the ordering of activation foci is arbitrary. Although the ordering of words within a document is obviously important, the ordering of activation foci is not. Therefore the author-topic model is arguably more suitable for meta-analysis than topic discovery from documents.

Estimating the model parameters

Given a collection of experiments with their associated activation coordinates and task categories, as well as the number of cognitive components K, the probabilities θ and β can be estimated using various algorithms, such as Gibbs sampling (Rosen-Zvi et al. 2010), expectation-maximization (EM) algorithm (Yeo et al., 2015) or collapsed variational Bayes (CVB) algorithm (Ngo et al., 2016). Both the EM (Yeo et al., 2015) and CVB (Ngo et al., 2016) algorithms were significantly faster than the Gibbs sampling algorithm (Rosen-Zvi et al., 2010).

The EM algorithm iterates between the E-step and M-step till convergence. In the E-step, the posterior distribution of each activation focus being generated from a latent task and component is estimated using the current estimates of θ and β. In the M-step, the estimated posterior distribution from the E-step is used to update θ and β. By contrast, the CVB algorithm avoids this two-step procedure by using the current estimate of the posterior distribution to update the posterior distribution. This is achieved by marginalizing (collapsing) the model parameters θ and β (hence the

name of the algorithm). By avoiding using point estimates of the model parameters θ and β to update the posterior distribution, the CVB algorithm might result in better parameter estimates than EM. While the EM and CVB algorithms worked equally well in large-scale datasets (Ngo et al., 2016), the CVB algorithm is more robust to the choice of hyperparameters in smaller datasets. Therefore the CVB algorithm was used in the present work.

Although the CVB algorithm for the author-topic model was first introduced in a conference article (Ngo et al., 2016), detailed derivations have not been published. Detailed derivations of the author-topic CVB algorithm are provided in Appendix A2. Explanations of why the CVB algorithm is theoretically better than the EM algorithm and standard variational Bayes inference are found in Appendix A3. In this work, Bayesian information criterion (BIC) is used to estimate the optimal number of cognitive components (Appendix A4). Further implementation details are found in Appendix A5.

Activation Foci of Experiments Involving Self-Generated Thought

To explore cognitive components subserving self-generated thought, we considered 1812 activation foci from 179 experimental contrasts across 167 imaging studies, each employing one of seven task categories subjected to prior meta-analysis with GingerALE (Fox and Lancaster, 2002; Laird et al., 2009, 2011; Fox et al., 2014; http://brainmap.org/ale). Of the 167 studies, 48 studies employed "Autobiographical Memory" (N = 19), "Navigation" (N = 13) or "Task Deactivation" (N = 16) tasks. The 48 studies were employed in a previous meta-analysis examining the default network (Spreng et al., 2009). There were 79 studies involving "Story-based Theory of Mind" (N = 18), "Nonstory-based Theory of Mind" (N = 42) and "Narrative Comprehension" (N = 19) tasks. The 79 studies were utilized in a previous meta-analysis examining social cognition and story comprehension (Mar et al., 2011). Finally, there were 40 studies involving the "Moral Cognition" task that was again utilized in a previous meta-analysis (Sevinc and Spreng, 2014). All foci coordinates were in or transformed to the MNI152 coordinate system (Lancaster et al., 2007).

Discovering Cognitive Components of Self-Generated Thought

The application of the author-topic model to discover cognitive components subserving self-generated thought (Figure 2) is conceptually similar to the original

application to the BrainMap (Yeo et al., 2015). The key difference is that the current application is restricted to seven related tasks in order to discover heterogeneity within a single functional domain, while the original application sought to find common and distinct cognitive components across domains.

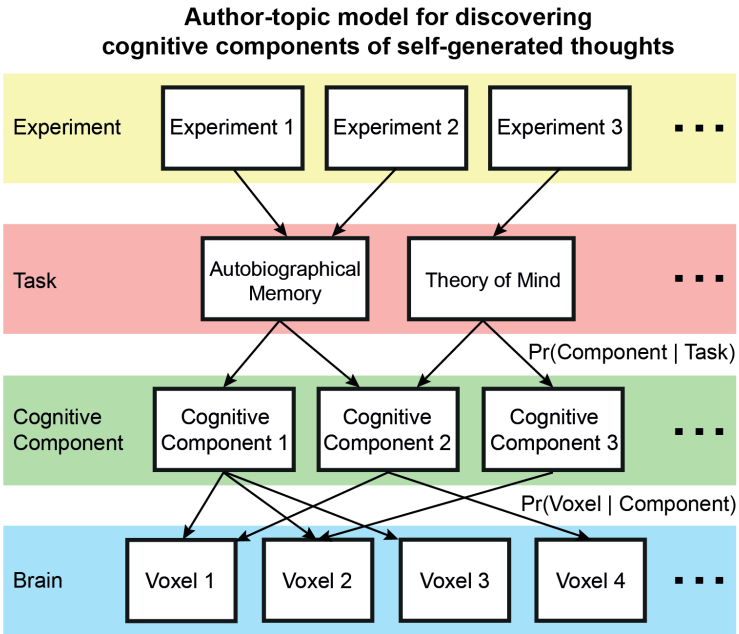

Figure 2. Author-topic model for discovering cognitive components of self-generated thought. The application of the author-topic model in this scenario is conceptually the same as the original application to the Brainmap database (Yeo et al., 2015). The key difference is the current focus on a narrow set of tasks within the functional domain of self-generated thought.

The model parameters are the probability of a task recruiting a component (Pr(component | task)) and the probability of a component activating a brain voxel (Pr(voxel | component)). The parameters were estimated from the 1812 activation foci from the previous section using the CVB algorithm (Appendices A2 and A5). BIC was used to estimate the optimal number of cognitive components (Appendix A4).

Interpreting Cognitive Components of Self-Generated Thought

The matrix Pr(voxel | component), β, can be interpreted as K brain images in MNI152 coordinate system (Lancaster et al., 2007), where K is the number of cognitive components. Volumetric slices highlighting specific subcortical structures were displayed using FreeSurfer (Fischl, 2012). The cerebral cortex was visualized by transforming the volumetric images from MNI152 space to fs_LR surface space using

Connetome Workbench (Van Essen et al., 2013) via the FreeSurfer surface space (Buckner et al., 2011; Fischl et al., 2012). For visualization purpose, isolated surface clusters with less than 20 vertices were removed, Pr(component | task) was thresholded at 1/K, and Pr(voxel | component) was thresholded at 1e-5, consistent with previous work (Yeo et al., 2015).

Activation Foci of Experiments Activating the Inferior Frontal Junction (IFJ)

To explore co-activation patterns expressed by the IFJ, we considered activation foci from experiments reporting activation within a left IFJ seed region (Figure S1). The IFJ seed region was delineated by a previous co-activation-based parcellation of the left inferior frontal suclus and the adjacent parts of the pre-central, inferior frontal, and middle frontal gyri (Muhle-Karbe et al. 2015). The seed region is publicly available on ANIMA (Reid et al. 2016; http://anima.fz-juelich.de/studies/MuhleKarbe_2015_IFJ). We selected experiments from the BrainMap database with at least one activation focus falling within the IFJ seed region. We further restricted our analyses to experimental contrasts involving normal subjects. Overall, there were 323 experiment contrasts from 323 studies with a total of 5201 activation foci.

Discovering Co-activation Patterns Involving the IFJ

To apply the author-topic model to discover co-activation patterns, we consider each of the 323 experimental contrasts to employ its own unique task category (Figure 3). The premise of the model is that the IFJ expresses one or more overlapping co-activation patterns depending on task contexts. A single experiment activating the IFJ might recruit one or more co-activation patterns. The model parameters are the probability that an experiment would recruit a co-activation pattern (Pr(co-activation pattern | experiment)), and the probability that a voxel would be involved in a co-activation pattern (Pr(voxel | co-activation pattern)). The parameters were estimated from the 5201 activation foci from the previous section using the CVB algorithm (Appendices A2 and A5). BIC was used to estimate the optimal number of cognitive components (Appendix A4).

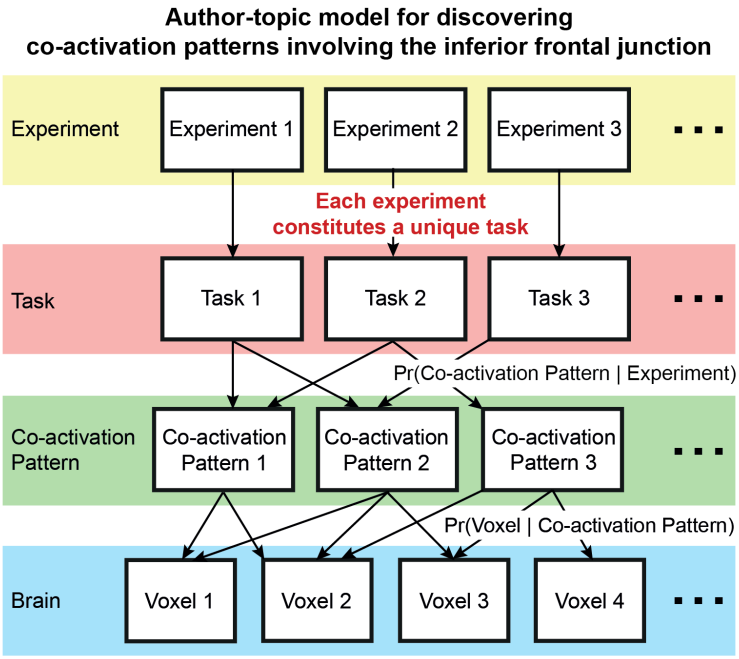

Figure 3. Author-topic model for discovering co-activation patterns involving the inferior frontal junction (IFJ). In contrast to Figure 1, this instantiation of the model assumes that each experiment employs a unique task category. The premise is that the IFJ expresses one or more overlapping co-activation patterns. A single experiment activating the IFJ might recruit one or more co-activation patterns.

Interpreting Co-activation Patterns of the IFJ

Similar to the previous application on self-generated thought, the matrix Pr(voxel | co-activation pattern), β, was visualized as K brain images in both fsLR surface space and MNI152 volumetric space. Like before, isolated surface clusters with less than 20 vertices were removed for the purpose of visualization.

Because each of the 323 experiments was treated as employing a unique task category, Pr(co-activation pattern | experiment), θ, is a matrix of size K x 323. θ was further mapped onto BrainMap task categories to assist in the interpretation. More specifically, since the experiments were extracted from the BrainMap database, so each experiment was tagged with one or more BrainMap task categories (Table S1). The Pr(co-activation pattern | experiment) was averaged across experiments employing the same task category to estimate the probability that a task category would recruit a co-activation pattern (Pr(co-activation pattern c | task t)). Further details of this procedure are found in Appendix A6.

Results

Cognitive Components of Self-Generated Thought

Figure 4a shows the BIC score as a function of the number of estimated cognitive components. A higher BIC score indicates a better model. Because the 2-component estimate achieved the highest BIC score, subsequent results will focus on the 2-component estimate.

The 2-component estimate is shown in Figure 4b. The seven tasks recruited the two cognitive components to different degrees. The top tasks recruiting component C1 were "Navigation" and "Autobiographical Memory". In contrast, the top tasks recruiting component C2 were "Narrative Comprehension", "Theory of Mind (nonstory-based)", "Theory of Mind (story-based)", and "Moral Cognition". "Task deactivation" recruited both components almost equally: 0.47 for component C1 and 0.53 for component C2.

The two cognitive components appeared to activate different portions of the default network (Figure 4b). Focusing our attention to the medial cortex, both components had high probability of activating the medial parietal cortex. However, while component C2's activation was largely limited to the precuneus, component C1's activation also included the posterior cingulate and retrosplenial cortices in addition to the precuneus. Both components also had high probability of activating the medial prefrontal cortex (MPFC). However, component C1's activations were restricted to the middle portion of the MPFC, while component C2's activations were restricted to the dorsal and ventral portions of the MPFC. Finally, component C1, but not component C2, had high probability of activating the hippocampal complex.

Switching our attention to the lateral cortex, component C1 had high probability of activating the posterior inferior parietal cortex, while component C2 had high probability of activating the entire stretch of cortex from the temporo-parietal junction to the temporal pole. Component C2, but not component C1, had high probability of activating the inferior frontal gyrus.

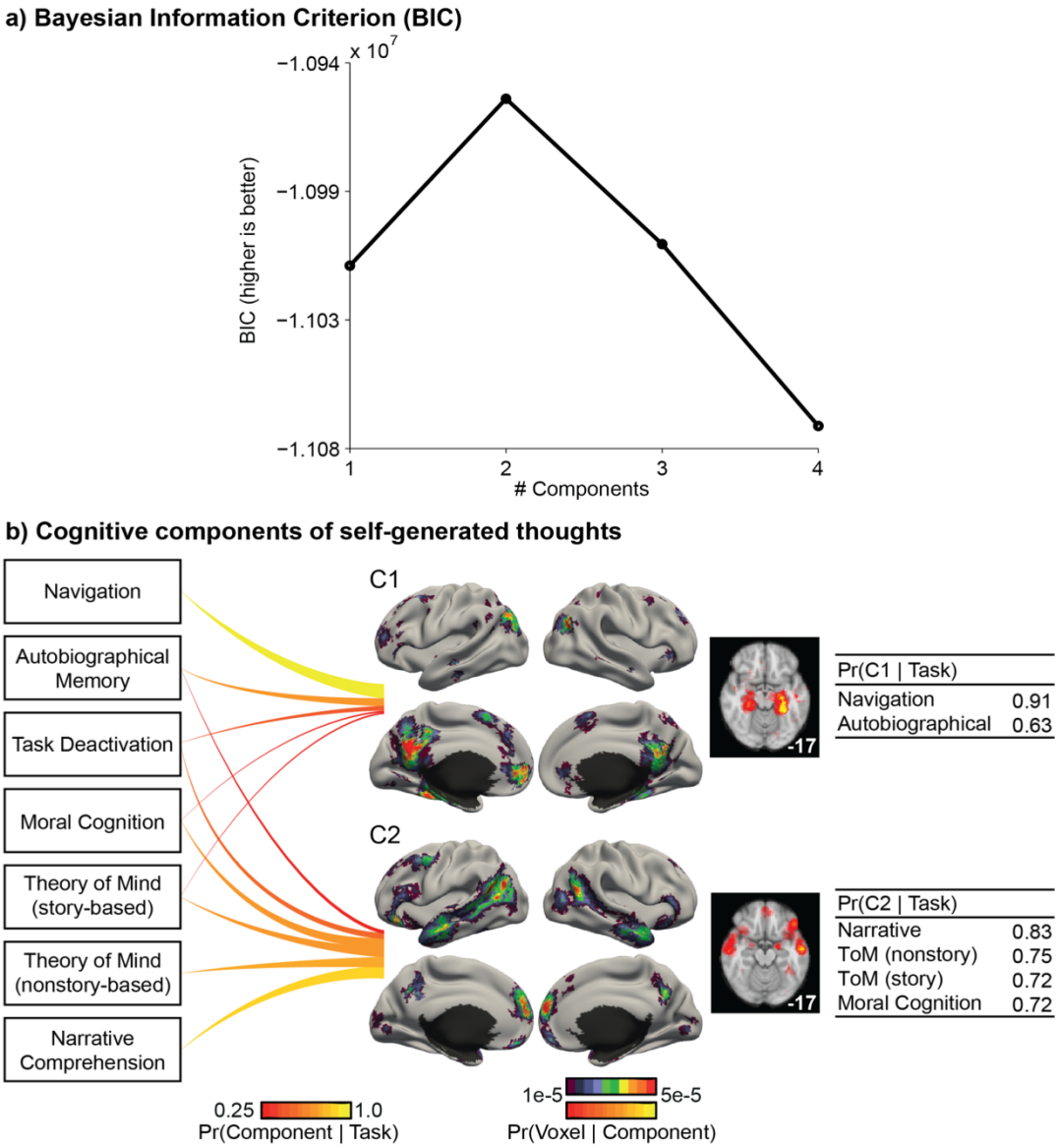

Figure 4. Cognitive components of self-generated thought. (a) Bayesian Information Criterion (BIC) plotted as a function of the number of estimated cognitive components. A higher BIC indicates a better model. BIC peaks at 2 components. (b) 2-component model estimate. The seven tasks recruit two cognitive components to different degrees. Each orange line connects 1 task with 1 component. The thickness and brightness of the lines are proportional to the magnitude of Pr(component | task). For each component, Pr(voxel | component) is visualized both on surface and in the volume. The top color bar is utilized for the surface-based visualization, whereas the bottom color bar is utilized for the volumetric slices. The tables on the right show the top tasks most likely to recruit a particular component. Task deactivation recruits the two components almost equally, and so is not assigned to any component in the tables.

Co-activation Patterns Involving the Inferior Frontal Junction (IFJ)

Figure 5a shows the BIC score as a function of the number of estimated co-activation patterns. Because the 3-pattern estimate achieved the highest BIC score, subsequent results will focus on the 3-pattern estimate.

The 3 estimated co-activation patterns are shown in Figure 5b. Not surprisingly, all three co-activation patterns involved the IFJ, but were generally spatially distinctive. Co-activation pattern C1 is left lateralized and might be recruited in tasks involving language processing. Co-activation pattern C2 involves bilateral superior parietal and posterior medial frontal cortices, and might be recruited in tasks involving attentional control. Co-activation pattern C3 involves bilateral frontal cortex, anterior insula and posterior medial frontal cortex, and might be recruited in tasks involving inhibition or response conflicts.

We now discuss in detail spatial differences among the co-activation patterns. Co-activation pattern C3 strongly engaged bilateral anterior insula, while co-activation pattern C1 only engaged left anterior insula. Co-activation pattern C2 did not engage the anterior insula.

In the frontal cortex, co-activation pattern C1 had high probability of activating the left inferior frontal gyrus, while co-activation pattern C3 had high probability of activating bilateral dorsal lateral prefrontal cortex. Although all three co-activation patterns also had high probability of activating the posterior medial frontal cortex (PMFC), the activation shifted anteriorly from co-activation patterns C1 to C2 to C3. In addition, the PMFC activation was left lateralized in C1, but bilateral in C2 and C3.

In the parietal cortex, co-activation pattern C2 included the superior parietal lobule and the intraparietal sulcus in both hemispheres. The activation was weaker in C3 and mostly concentrated in the intraparietal sulcus, while C1 did not activate the parietal cortex.

Finally, co-activation pattern C1 engaged bilateral superior temporal cortex, which might overlap with early auditory regions. Both co-activation patterns C1 and C2 also had high probability of activating ventral visual regions, especially in the fusiform gyrus.

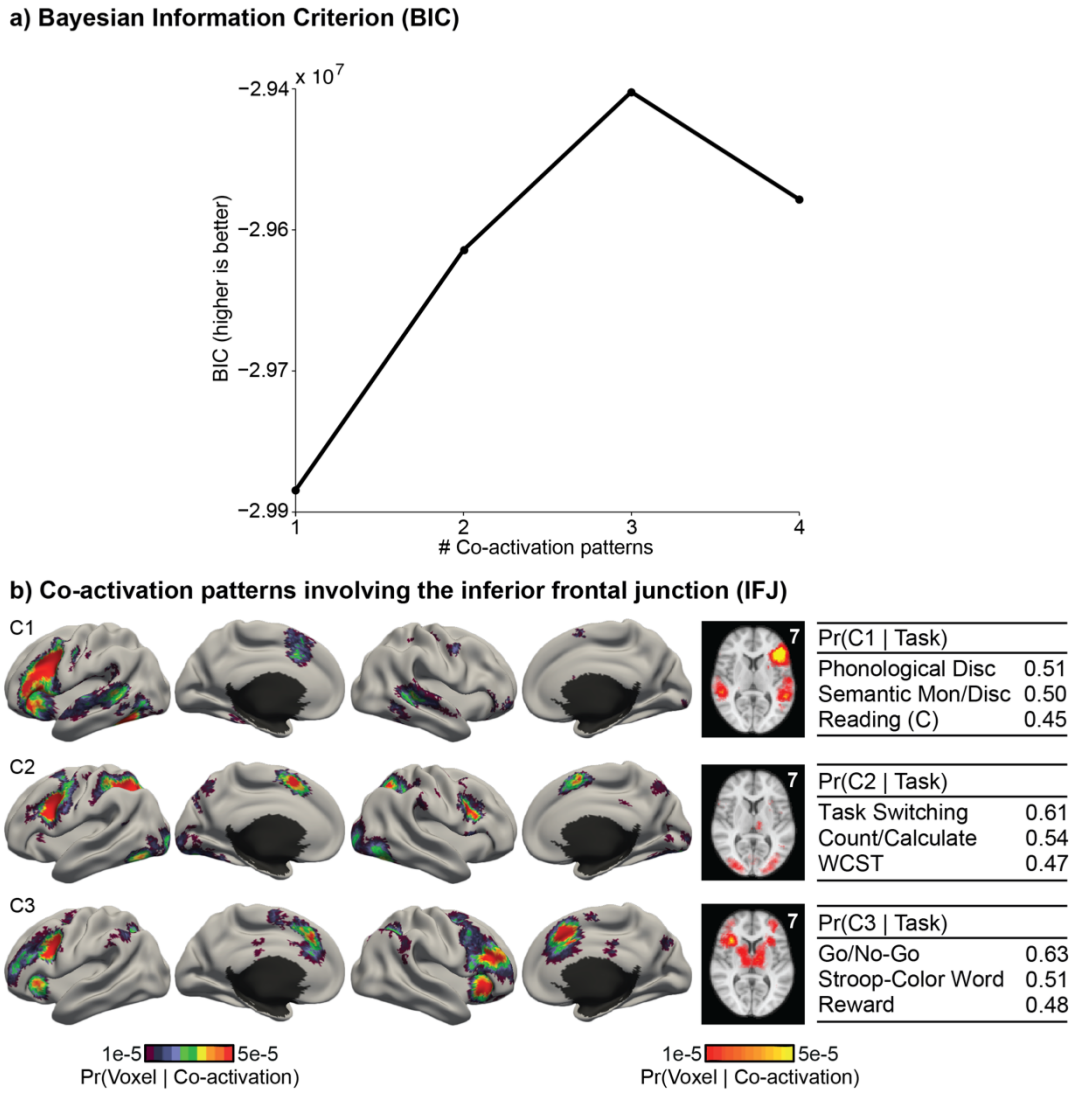

Figure 5. Co-activation patterns involving the inferior frontal junction (IFJ). (a) Bayesian Information Criterion (BIC) plotted as a function of the number of estimated co-activation patterns. A higher BIC indicates a better model. BIC peaks at 3 co-activation patterns. (b) Estimate of 3 co-activation patterns. For each co-activation pattern, Pr(voxel | co-activation pattern) is visualized both on surface and in the volume. The tables on the right show the top tasks most likely to recruit a particular component based on the posthoc estimate of Pr(co-activation pattern | task). "(C)" and "(O)" indicate "covert" and "overt" respectively. "Mon/Disc" is short for "Monitoring/Discrimination". "Count/Calculate" is short for "Counting/Calculation". "WCST" is short for "Wisconsin Card Sorting Test".

The top three tasks recruiting each co-activation pattern is shown in Figure 5b. The top tasks with the highest probability of recruiting co-activation C1 were "Phonological Discrimination", "Semantic Monitoring/Discrimination", and "Covert Reading". The top tasks recruiting co-activation C2 were "Task Switching", "Counting/Calculation", and "Wisconsin Card Sorting Task". The top tasks recruiting

co-activation C3 were “Go/ No-Go”, “Stroop – Color Word”, and “Reward”. For completeness, the top five tasks recruiting each co-activation pattern are shown in Table S2.

To help interpret the results, Table S3 lists the top three experiments with the highest Pr(co-activation pattern | experiment) for each of the top three tasks associated with each co-activation pattern. For example, Table S3-A lists the top three experiments employing “Phonological Discrimination” with the highest Pr(co-activation pattern C1 | experiment), Table S3-B lists the top three experiments employing “Semantic Monitoring/Discrimination” with the highest Pr(co-activation pattern C2 | experiment), and Table S3-C lists the top three experiments employing “Covert Reading” with the highest Pr(co-activation pattern C3 | experiment).

Table 1: Spatial locations of co-activation patterns within the IFJ

	x/ mm	y/ mm	z/ mm
Co-activation pattern C1	-39.60 (3.41)	5.60 (4.53)	30.70 (3.65)
Co-activation pattern C2	-39.44 (2.07)	6.56 (5.73)	29.78 (3.93)
Co-activation pattern C3	-38.67 (4.64)	5.67 (4.33)	30.89 (4.28)

Each row of the table shows the mean and standard deviation of the coordinates of the activation foci within the IFJ reported by the top 3 experiments that have the highest probabilities of recruiting a co-activation pattern (Pr(co-activation pattern | experiment)) and employing at least one of the top 3 tasks with the highest probabilities of recruiting the co-activation pattern (Pr(co-activation pattern | task)). See Figure S2 for volumetric slices illustrating the locations of the activation foci within the IFJ. Across the 3 co-activation patterns, the mean coordinates do not differ by more than 1.5mm in any dimension, suggesting that the co-activation patterns were not fractionating the IFJ.

Although previous analyses using co-activation based parcellation and MACM (Muhle-Karbe et al., 2015) suggested the IFJ seed region to be a single functional unit, one might be concerned that the co-activation patterns (Figure 5b) might simply be further fractionating the IFJ into sub-regions. Figure S2 illustrates the activation foci of the top three experiments with the highest Pr(co-activation pattern | experiment) for each of the top three tasks associated with each co-activation pattern falling inside the IFJ. Table 1 shows the mean and standard deviation of the coordinates of these activation foci for each co-activation pattern. The mean locations of the IFJ activations across co-activation patterns did not differ by more than 1.5mm along any dimension, suggesting that the co-activation patterns were probably not simply sub-dividing the IFJ.

Discussion

The author-topic model can encode the intuitive notion that behavioral tasks recruited multiple cognitive components, supported by multiple brain regions (Mesulam 1990; Poldrack 2006; Barrett & Satpute, 2013). We have previously utilized the author-topic model for large-scale meta-analysis across functional domains (Yeo et al., 2015; Bertolero et al., 2015). By exploiting a recently developed CVB algorithm for the author-topic model (Ngo et al., 2016), we show that the model can also be utilized for small-scale meta-analyses focusing on a given functional domain or brain seed region.

A dominant approach for small-scale meta-analyses is ALE, which seeks to find consistent activations across neuroimaging experiments within a functional domain or mental disorder or seed region (also known as MACM). ALE treats heterogeneity across experiments as noise. By contrast, the author-topic model evaluates whether the heterogeneity might be indicative of robust latent patterns within the data. We applied the author-topic model to two applications: one on fractionating a functional sub-domain and one on discovering multiple task-dependent co-activation patterns.

In the first application, the author-topic model encoded the notion that tasks involving self-generated thought might recruit one or more spatially overlapping. cognitive components. The model revealed two cognitive components that appeared to delineate two overlapping default sub-networks, consistent with the hypothesized functional organization of the default network (Andres-Hanna et al., 2014). In the second application, the author-topic model encoded the notion that experiments activating the IFJ might recruit one or more co-activation patterns dependent on task contexts. The model revealed that the IFJ participated in three co-activation patterns, suggesting that IFJ flexibly co-activate with different brain regions depending on the cognitive demands of different tasks. Overall, our work suggests that the author-topic model is a versatile tool suitable for both small-scale and large-scale meta-analyses.

Cognitive components of self-generated thought

Self-generated thought is a heterogeneous set of cognitive processes that includes inferring other people's mental states, dealing with challenging moral scenarios, understanding narratives, retrieving autobiographical memories, internalizing semantic information, and mind-wandering. These processes are

characterized by an absence of external stimuli, self-related, and often involve simulation or inferential reasoning (Buckner et al., 2008; Spreng et al. 2009; Smallwood et al., 2011; Baird et al., 2011; Prebble at al. 2013; Smallwood, 2013). Studies of tasks involving self-generated thought have consistently found the activation of the default network, suggesting its functional importance (Buckner et al. 2008; Spreng et al. 2009; Andrews-Hanna et al., 2010; Andrews-Hanna, 2012; Gorgolewski, 2014; Callard and Margulies, 2014). Additionally, the default network has been fractionated into sub-networks supporting different aspects of these stimulus independent cognitive processes (Buckner et al., 2008; Uddin et al. 2009; Sestieri et al., 2011; Andrews-Hanna et al., 2010; Kim, 2012; Seghier and Price, 2012; Salomon et al., 2013; Bzdok et al., 2013).

The author-topic model revealed two cognitive components of self-generated thought that appeared to fractionate the default network (Figure 4). The default network has been defined as the set of brain regions that are more active during passive task conditions relative to active task conditions, i.e., task deactivation (Shulman et al., 1997; Buckner et al., 2008). Our results show that "Task Deactivation" recruited both components with almost equal probability, suggesting that rest is a task that reliably engages both sub-components of the default network. While there have been multiple studies fractionating the default network (Andrews-Hanna et al., 2010; Mayer et al. 2010; Yeo et al. 2011; Kim, 2012; Humphreys et al., 2015), the specific patterns of fractionation have differed across studies. The spatial topography of components C1 and C2 in this paper corresponded well to the previously proposed "medial temporal subsystem" and "dorsal medial subsystem" respectively (Figure 3A of Andrews-Hanna et al. 2014; Andrews-Hanna et al., 2010).

The first cognitive component C1 was strongly recruited by navigation and autobiographical memory tasks, suggesting its involvement in constructive mental simulation based upon mnemonic content (Andrews-Hanna et al., 2014). Constructive mental simulation is the process of combining information from the past in order to create a novel mental representation, such as imagining the future (Buckner and Carroll, 2007; Hassabis and Maguire, 2007; Schacter et al., 2007). "Navigation" tasks require constructive mental simulation to create a mental visualization ("scene construction") for planning new routes and finding ways in unfamiliar contexts (Burgess et al., 2002; Byrne et al. 2007). On the other hand, "Autobiographical Memory" tasks require constructive mental simulation to project past experience

("constructive episodic simulation"; Atance and O'Neil, 2001; Schacter et al. 2007) or previously acquired knowledge ("semantic memory"; Irish et al., 2012; Brown et al. 2014) across spatiotemporal scale to enact novel perspectives. Overall, cognitive component C1 seems to support the projection of self, events, experiences, images and knowledge to a new temporal or spatial context based upon an associative constructive process, likely mediated by the hippocampus and connected brain structures (Moscovitch et al. 2016, Christoff et al., 2016).

The second cognitive component C2 was strongly recruited by narrative comprehension and theory of mind, suggesting its involvement in mentalizing, inferential, and conceptual processing (Andrews-Hanna et al., 2014). Mentalizing is the process of monitoring one's own mental states or predicting others' mental states (Frith and Frith 2003), while conceptual processing involves internalizing and retrieving semantic or social knowledge (Binder and Desai, 2011; Overwalle, 2009). "Narrative Comprehension" engages conceptual processing to understand the contextual settings of the story, and requires mentalizing to follow and infer the characters' thoughts and emotions (Gernsbacher et al., 1998; Mason et al. 2008). "Theory of Mind" tasks require the recall of learned knowledge, social norms and attitudes to form a meta-representation of the perspectives of other people (Leslie, 1987; Frith and Frith, 2005; Binder and Desai, 2011). The grouping of Narrative Comprehension and Theory of Mind tasks echoes the link between the ability to comprehend narratives and the ability to understanding others' thoughts in developmental studies of children (Guajardo and Watson, 2001; Slaughter et al. 2007; Mason et al. 2008).

The two cognitive components had high probability of activating common and distinct brain regions. Both components engaged the posterior cingulate cortex and precuneus, which are considered part of the "core" sub-network that subserves personally relevant information necessary for both constructive mental simulation and mentalizing (Andrews-Hanna et al. 2014). The distinct brain regions supporting each cognitive component also corroborated the distinct functional role of each component. For instance, component C1, but not C2, had high probability of activating the medial temporal lobe and hippocampus. This is consistent with neuropsychological literaure (Hassabis et al., 2007; Rosenbaum et al., 2007; Race et al., 2011; Rosenbaum et al., 2009) showing that patients with impairment of the medial temporal lobe and hippocampus retain theory of mind and narrative construction capabilities, while

suffering deficits in episodic memories and imagining the future (Hassabis et al., 2007; Rosenbaum et al., 2007; Race et al., 2011; Rosenbaum et al., 2009).

Co-activation patterns of the IFJ

The inferior frontal junction (IFJ) is located in the prefrontal cortex at the intersection between the inferior frontal sulcus and the inferior precentral sulcus (Brass et al., 2005; Derfuss et al., 2005). The IFJ has been suggested to be involved in a wide range of cognitive functions, including task switching (Brass and Cramon, 2002; Derfuss et al., 2005), attentional control (Asplund et al. 2010; Baldauf and Desimone, 2014), detection of conflicting responses (Chikazoe et al. 2009; Levy and Wagner, 2011), short-term memory (Zanto et al. 2010; Sneve et al. 2013), construction of attentional episodes (Duncan, 2013) and so on. Using the author-topic model, we found that the IFJ participated in three task-dependent co-activation patterns.

Co-activation pattern C1 might be involved in some aspects of language processing, such as phonological processing for lexical understanding. Phonological processing is an important linguistic function, concerning the use of speech sounds in handling written or oral languages (Wagner and Torgesen 1987; Poldrack et al. 1999; Friederici 2002). The top tasks associated with C1 were "Phonological Discrimination", "Semantic Monitoring/ Discrimination" and "Covert Reading" (Figure 5b). Inspecting the top three experiments recruiting these three tasks (Table S3) offered more insights into the functional characteristics of co-activation pattern C1. The top "Phonological Discrimination" experiments with the highest probability of recruiting co-activation pattern C1 examined phonological assembly/disassembly (Tyler et al., 2005) and phonological representation (Xu et al. 2001). Among "Semantic Monitor/Discrimination" experiments, C1 was associated with an experiment requiring lexical perception and not just perception of elementary sounds (Poeppei et al., 2004), as well as experiments demanding retrieval of semantic meaning (Wagner et al. 2001). The top "Covert Reading" experiments most strongly associated with C1 identified a common brain network activated by both reading and listening (Jobard et al., 2007), as well as language comprehension across different media (Small et al., 2009), suggesting the involvement of C1 in generic language comprehension. The language and phonological processing interpretation is supported by C1's strong left lateralization with high probability of activating classical auditory

and language brain regions, including the left (but not right) inferior frontal gyrus and bilateral superior temporal cortex.

Co-activation pattern C2 might be engaged in attentional control, especially aspects of task maintenance and shifting of attentional set. Attentional set-shifting is the ability to switch between mental states associated with different reactionary tendencies (Omori et al. 1999, Konishi et al. 1998). The top three tasks most highly associated with C2 were "Task Switching", "Counting/Calculation" and "Wisconsin Card Sorting Test" (Figure 5b). Inspecting the top three experiments under the top task paradigms provided further insights into the functional characteristics of co-activation pattern C2 (Table S3). The top "Task Switching" experiments most strongly associated with C2 involved the switching of mental states to learn new stimulus-response or stimulus-outcome associations (Xue et al. 2008; Sylvester et al. 2003; Omori et al. 1999). Furthermore, the top "Counting/ Calculation" experiments most strongly recruiting co-activation pattern C2 involved switching of resolution strategies in executive function. For example, one experimental contrast seeks to isolate demanding mental calculation but not retrieval of numerical facts (Zago et al. 2001; Pesenti 2005), suggesting C2's involvement in the selection and application of strategies to solve arithmetic problems. C2 was also strongly expressed by "Wisconsin Card Sorting Task" (WCST) experiments, which required attentional set-shifting to change behavioral patterns in reaction to changes of perceptual dimension (color, shape, or number) upon which the target and reference stimuli were matched (Berman 1995; Konishi 2002; Konishi 2003). Overall, the attentional control interpretation of co-activation pattern C2 is supported by C2's high probability of activating classical attentional control regions, such as the superior parietal lobule and the intra-parietal sulcus, although there is a clear lack of DLPFC activation.

Co-activation pattern C3 might be engaged in inhibition or response conflict resolution. Conflict-response resolution is a central aspect of cognitive control, which involves monitoring and mediating incongruous response tendencies (Pardo et al. 1990; Braver et al. 2001; Barch et al. 2001). Co-activation pattern C3 is most strongly recruited by experiments utilizing "Go/No-Go", "Stroop – Color Word" and "Reward" tasks (Figure 5b). Closer examination of the top three experiments under each task paradigm provided further insights into the functional characteristics of C3 (Table S3). The top experiments utilizing "Go/No-Go" required the monitoring, preparing and reconciling of conflicting tendencies to either giving a "go" or "stop"

(no-go) response (Chikazoe et al. 2009, Simoes-Franklin et al. 2010; Zandbelt et al. 2011). The top "Stroop" experiments most strongly associated with C3 required control over the tendencies to either read the stimulus word or to name its color (Pompei et al. 2011; Weiss et al. 2003). Finally, it might be surprising at first glance that the "Reward" task was grouped together with "Go/No-Go" and "Stroop" tasks. However, the top experiments utilizing the "Reward" task all required subjects to make competing decisions (Table S3). For examples, these experiments involved making decisions of selling versus buying an item (Knutson et al. 2008) or choosing between immediate but smaller rewards versus later but larger ones (Peters et al. 2010). Overall, the inhibition or response conflict interpretation of co-activation pattern C3 is supported by C3's high probability of activating classical executive function regions, including the bilateral dorsal lateral prefrontal cortex.

The intriguing location of the IFJ and its functional heterogeneity suggests the role of IFJ as an integrative hub for different cognitive functions. For example, the IFJ has been suggested to consolidate information streams for cognitive control from its bordering brain regions (Brass et al., 2005). The involvement of the IFJ in three task-dependent co-activation patterns supported the view that the IFJ orchestrates different cognitive mechanisms to allow their operations in harmony.

Conclusion

Heterogeneities across neuroimaging experiments are often treated as noise in coordinate-based meta-analyses. Here we demonstrate that the author-topic model can be utilized to determine if the heterogeneities can be explained by a small number of latent patterns. In the first application, the author-topic model revealed two overlapping cognitive components subserving self-generated thought. In the second application, the author-topic revealed the participation of the IFJ in three task-dependent co-activation patterns. These applications exhibited the broad utility of the author-topic model, ranging from discovering functional subdomains or task-dependent co-activation patterns. Code from this study is publicly available at GITHUB_LINK_TO_BE_ADDED.

Acknowledgements

This work was supported by Singapore MOE Tier 2 (MOE2014-T2-2-016), NUS Strategic Research (DPRT/944/09/14), NUS SOM Aspiration Fund (R185000271720), Singapore NMRC (CBRG/0088/2015), NUS YIA and the Singapore National Research Foundation (NRF) Fellowship (Class of 2017). Simon Eickhoff is supported by the National Institute of Mental Health (R01-MH074457), the Helmholtz Portfolio Theme "Supercomputing and Modeling for the Human Brain" and the European Union's Horizon 2020 Research and Innovation Programme under Grant Agreement No. 7202070 (HBP SGA1). Comprehensive access to the BrainMap database was authorized by a collaborative-use license agreement (http://www.brainmap.org/collaborations.html). BrainMap database development is supported by NIH/NIMH R01 MH074457.

Appendix

A1. Mathematical Model

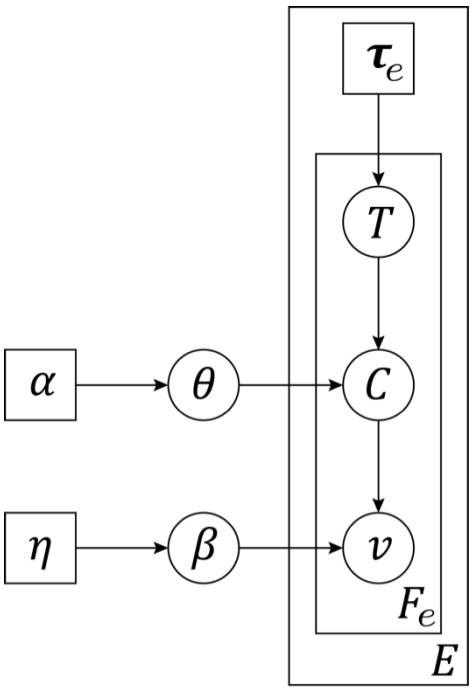

Figure 6. Formal graphical representation of the author-topic model for coordinate-based meta-analysis (Yeo et al. 2015). The circles represent random variables, while the squares represent non-random parameters. The edges represent statistical dependencies. There are E experiments. The e-th experiment utilizes a set of behavioral tasks $\boldsymbol{\tau}_e$ and reports F_e number of activated voxels. The f-th activated voxel has an observed location v, and associated with a latent (unobserved) component C and a latent (unobserved) task $T \in \boldsymbol{\tau}_e$. The variables at the corners of the rectangles (plates) indicate the number of times the variables within the rectangles were replicated. Therefore $\boldsymbol{\tau}_e$ was replicated E times, once for each experiment. For the e-th experiment, the variables v, C and T were replicated F_e times, once for each activated voxel. θ denote Pr(component | task) and β denote Pr(voxel | component). Thus θ and β are matrices, where each row is a categorical distribution summing to one. α and η are hyperparameters parameterizing the Dirichlet priors on θ and β respectively.

Figure 6 shows the formal graphical representation of the author-topic model for coordinate-based meta-analysis. The model assumes that there are E experiments. The e-th experiment is associated with a set of tasks $\boldsymbol{\tau}_e$ and an unordered set $\boldsymbol{v}_e$ of F_e activated voxels. The location of the f-th activated voxel is denoted as v_{ef}, corresponding to one of $V = 284100$ possible locations in MNI152 2mm space (Lancaster et al., 2007). The collection of activated voxels across all E experiments is denoted as $\boldsymbol{v} = \{\boldsymbol{v}_e\}$. The collection of tasks across all E experiments is denoted as $\boldsymbol{\tau} = \{\boldsymbol{\tau}_e\}$. Thus, $\{\boldsymbol{v}, \boldsymbol{\tau}\}$ are the input data for the meta-analysis.

We assume that there are K cognitive components and M unique tasks in the dataset. For example, M = 83 in Yeo et al. (2015). Each task has a certain (unknown) probability of recruiting a component Pr(component | task). The collection of all probabilities Pr(component | task) is denoted by a $M \times K$ matrix θ. The t-th row and k-th column of θ corresponds to the probability of the t-th task recruiting the k-th component. Each component has a certain (unknown) probability of activating a voxel pr(voxel | component). The collection of all probabilities Pr(voxel | component) is denoted by a $K \times V$ matrix β. The k-th row and v-th column of β corresponds to the probability of the k-th component activating the v-th MNI152 voxel. Symmetric Dirichlet priors with hyperparameter α are assumed on θ, and hyperparameter η on β.

We assume that the activated voxels of an experiment are independent and identically distributed (conditioned on knowing θ and β). To generate the f-th activated voxel v_{ef} in the e-th experiment, a task T_{ef} is sampled uniformly from the set of tasks $\boldsymbol{\tau}_e$ utilized by the experiment. Given task T_{ef}, a component C_{ef} is sampled based on the probability that the task would recruit a component (corresponding to the T_{ef}-th row of the θ matrix). Given component C_{ef}, the activation location v_{ef} is sampled based on the probability that the component would activate a voxel (corresponding to the C_{ef}-th row of the β matrix). T_{ef} and C_{ef} are known as latent variables because they are not directly observed in the input data. We denote $\boldsymbol{T} = \{T_{ef}\}$, $\boldsymbol{C} = \{C_{ef}\}$ as the collection of latent tasks and components across all experiments and activated voxels.

Given the number of cognitive components K, the fixed hyperparameters α and η, and the activated voxels and behavioral task categories $\{\boldsymbol{v}, \boldsymbol{\tau}\}$ of all experiments, the parameters Pr(component | task) θ, and Pr(voxel | component) β can be estimated using different algorithms. Gibbs sampling was proposed in the original author-topic paper (Rosen-Zvi et al. 2010). We also proposed a faster expectation maximization (EM) algorithm that was highly efficient on large amount of data (Yeo et al. 2015). In the present work, we used collapsed variational Bayes (CVB) inference (Ngo et al. 2016), which is less sensitive to choice of hyperparameters compared to the EM algorithm.

A2. Collapsed Variational Bayes (CVB) Inference

The CVB algorithm for the latent dirichlet allocation model (Blei et al., 2006) was introduced by Teh et al. (2006). We subsequently extended the CVB algorithm to the author-topic model (Ngo et al. 2016). Here we provide the derivation of the algorithm in detail.

We start by following the standard variational Bayesian inference procedure (Beal, 2003) of constructing the lower bound of the log data likelihood:

$$\begin{aligned}
&\log p(\boldsymbol{v} \mid \alpha, \eta, \boldsymbol{\tau}) \\
&= \log \textstyle\sum_{\boldsymbol{C},\boldsymbol{T}} p(\boldsymbol{v}, \boldsymbol{C}, \boldsymbol{T} \mid \alpha, \eta, \boldsymbol{\tau}) \\
&= \log \textstyle\sum_{\boldsymbol{C},\boldsymbol{T}} q(\boldsymbol{C}, \boldsymbol{T}) \frac{p(\boldsymbol{v},\boldsymbol{C},\boldsymbol{T} \mid \alpha,\eta,\boldsymbol{\tau})}{q(\boldsymbol{C},\boldsymbol{T})} \\
&= \log E_{q(\boldsymbol{C},\boldsymbol{T})} \left(\frac{p(\boldsymbol{v},\boldsymbol{C},\boldsymbol{T} \mid \alpha,\eta,\boldsymbol{\tau})}{q(\boldsymbol{C},\boldsymbol{T})} \right) \\
&\geq E_{q(\boldsymbol{C},\boldsymbol{T})}(\log p(\boldsymbol{v}, \boldsymbol{C}, \boldsymbol{T} \mid \alpha, \eta, \boldsymbol{\tau})) - E_{q(\boldsymbol{C},\boldsymbol{T})}(\log q(\boldsymbol{C}, \boldsymbol{T}))
\end{aligned} \tag{1}$$

where $q(\boldsymbol{C}, \boldsymbol{T})$ can be any probability distribution and the inequality (Eq. (1)) utilizes the Jensen inequality (Beal, 2003). We can indirectly maximize the data likelihood $p(\boldsymbol{v} \mid \alpha, \eta, \boldsymbol{\tau})$ by finding the variational distribution $q(\boldsymbol{C}, \boldsymbol{T})$ that maximizes the lower bound (Eq. (1)). The equality in Eq. (1) occurs when $q(\boldsymbol{C}, \boldsymbol{T}) = p(\boldsymbol{C}, \boldsymbol{T} \mid \boldsymbol{v}, \alpha, \eta, \boldsymbol{\tau})$, i.e., when the variational distribution is equal to the true posterior distribution. However, computing the true posterior distribution of the latent variables is intractable because of dependencies among the variables constituting $\boldsymbol{C}$ and $\boldsymbol{T}$. Instead, the posterior of the latent variables $(\boldsymbol{C}, \boldsymbol{T})$ is approximated to be factorizable (Teh et al., 2006):

$$q(\boldsymbol{C}, \boldsymbol{T}) = \prod_{e=1}^{E} \prod_{f=1}^{F_e} q(C_{ef}, T_{ef}), \tag{2}$$

where $q(\boldsymbol{C}, \boldsymbol{T})$ is a categorical distribution with parameters ϕ:

$$q(C_{ef} = c, T_{ef} = t) = \phi_{efct} \quad . \tag{3}$$

By plugging Eq. (3) into Eq. (1), we get

$$\log p(\boldsymbol{v} \mid \alpha, \eta, \boldsymbol{\tau})$$
$$\geq E_{q(\boldsymbol{C},\boldsymbol{T})}[\log p(\boldsymbol{v}, \boldsymbol{C}, \boldsymbol{T} \mid \alpha, \eta, \boldsymbol{\tau})] - E_{q(\boldsymbol{C},\boldsymbol{T})}[\log q(\boldsymbol{C}, \boldsymbol{T})]$$
$$= \sum_{c=1}^{K} \sum_{t \in \boldsymbol{\tau}_e} \phi_{efct} \left(E_{q(\boldsymbol{C}_{-ef}, \boldsymbol{T}_{-ef})} \left(\log p \left(\boldsymbol{v}, \boldsymbol{C}_{-ef}, \boldsymbol{T}_{-ef}, C_{ef} = c, T_{ef} = t \mid \alpha, \eta, \boldsymbol{\tau} \right) \right) \right) - \sum_{e=1}^{E} \sum_{f=1}^{F_e} \sum_{c=1}^{K} \sum_{t \in \boldsymbol{\tau}_e} \phi_{efct} \log \phi_{efct}, \tag{4}$$

where the subscript "$-ef$" indicates the exclusion of corresponding variables C_{ef} and T_{ef}. Maximizing the lower bound (Eq. (4)) by differentiating with respect to ϕ and using the constraint that $\sum_{c=1}^{K} \sum_{t \in \boldsymbol{\tau}_e} \phi_{efct} = 1$, we get the update equation

$$\phi_{efct} = \frac{\exp \left(E_{q(\boldsymbol{C}_{-ef}, \boldsymbol{T}_{-ef})} \left(\log p \left(\boldsymbol{v}, \boldsymbol{C}_{-ef}, \boldsymbol{T}_{-ef}, C_{ef} = c, T_{ef} = t \mid \alpha, \eta, \boldsymbol{\tau} \right) \right) \right)}{\sum_{c'} \sum_{t' \in \boldsymbol{\tau}_e} \exp \left(E_{q(\boldsymbol{C}_{-ef}, \boldsymbol{T}_{-ef})} \left(\log p \left(\boldsymbol{v}, \boldsymbol{C}_{-ef}, \boldsymbol{T}_{-ef}, C_{ef} = c', T_{ef} = t' \mid \alpha, \eta, \boldsymbol{\tau} \right) \right) \right)}, \tag{5}$$

The CVB algorithm involves iterating Eq. (5) till convergence. The remaining derivations concern the evaluation of Eq. (5). We first apply the conditional independence assumptions of the author-topic model to simplify the joint probability distribution in Eq. (5):

$$\log p(\boldsymbol{v}, \boldsymbol{C}, \boldsymbol{T} \mid \alpha, \eta, \boldsymbol{\tau}) = \log p(\boldsymbol{v} \mid \boldsymbol{C}, \eta) + \log p(\boldsymbol{C} \mid \boldsymbol{T}, \alpha) + \log p(\boldsymbol{T} \mid \boldsymbol{\tau}). \tag{6}$$

By exploiting the properties of Dirichlet-multinomial compound distribution (Teh et al., 2006), the first term on the right hand side of Eq. (6) is given by

$$\log p(\boldsymbol{v} \mid \boldsymbol{C}, \eta)$$
$$\overset{(a)}{=} \log \prod_{c=1}^{K} \left[\frac{\Gamma(V\eta)}{\Gamma(V\eta + N_{\cdot\cdot c\cdot})} \prod_{v=1}^{V} \frac{\Gamma(\eta + N_{\cdot\cdot cv})}{\Gamma(\eta)} \right]$$
$$\overset{(b)}{=} \log \prod_{c=1}^{K} \left[\frac{1}{V\eta(V\eta + 1) \dots (V\eta + N_{\cdot\cdot c\cdot} - 1)} \prod_{v=1}^{V} \eta(\eta + 1) \dots (\eta + N_{\cdot\cdot cv} - 1) \right]$$
$$= -\sum_{c=1}^{K} \sum_{m=0}^{N_{\cdot\cdot c\cdot}-1} \log(V\eta + m) + \sum_{c=1}^{K} \sum_{v=1}^{V} \sum_{m=0}^{N_{\cdot\cdot cv}-1} \log(\eta + m), \tag{7}$$

where equality (7a) arises from the definition of the Dirichlet-multinomial compound distribution and $\Gamma(\cdot)$ is the Gamma function. N_{etcv} is the number of activation foci in experiment e generated by task t, cognitive component c, and located at brain location v. The dot '·' indicates that the corresponding variable is summed out. For example, $N_{\cdot\cdot c\cdot}$ is the number of activation foci generated by component c across all experiments. Equation (7b) arises from the identity $\Gamma(z+1) = z\Gamma(z)$ for $z > 0$. Using the same procedure, the second term on the right hand side of Eq. (6) can be written as

$$\log p(\boldsymbol{C} \mid \boldsymbol{T}, \alpha) = -\sum_{t \in \boldsymbol{\tau}} \sum_{m=0}^{N_{\cdot t\cdot\cdot}-1} \log(K\alpha + m) + \sum_{t \in \boldsymbol{\tau}} \sum_{c=1}^{K} \sum_{m=0}^{N_{\cdot tc\cdot}-1} \log(\alpha + m), \tag{8}$$

Substituting Eq. (7) and Eq. (8) back into Eq. (6), we get

$$\begin{aligned} &\log p(\boldsymbol{v}, \boldsymbol{C}, \boldsymbol{T} \mid \alpha, \eta, \boldsymbol{\tau}) \\ &\quad = -\sum_{c=1}^{K} \sum_{m=0}^{N_{\cdot\cdot c\cdot}-1} \log(V\eta + m) + \sum_{c=1}^{K} \sum_{v=1}^{V} \sum_{m=0}^{N_{\cdot\cdot cv}-1} \log(\eta + m) \\ &\quad - \sum_{t \in \boldsymbol{\tau}} \sum_{m=0}^{N_{\cdot t\cdot\cdot}-1} \log(K\alpha + m) + \sum_{t \in \boldsymbol{\tau}} \sum_{c=1}^{K} \sum_{m=0}^{N_{\cdot tc\cdot}-1} \log(\alpha + m) \\ &\quad + \log p(\boldsymbol{T} \mid \boldsymbol{\tau}). \end{aligned} \tag{9}$$

We are now ready to substitute Eq. (9) back into the update Eq. (5). The last term ($\log p(\boldsymbol{T} \mid \boldsymbol{\tau})$) of Eq. (9) exists in both the numerator and denominator of Eq. (5) and thus cancels out. The remaining terms in Eq. (9) can be similarly simplified as follows. For example, the first term of Eq. (9) can be written as

$$-\sum_{c=1}^{K} \sum_{m=0}^{N_{\cdot\cdot c\cdot}-1} \log(V\eta + m) = \left[-\sum_{c'=1}^{K} \sum_{m=0}^{N_{\cdot\cdot c'\cdot}^{-ef}-1} \log(V\eta + m) \right] - \log\left(V\eta + N_{\cdot\cdot c\cdot}^{-ef}\right). \tag{10}$$

Therefore when Eq. (9) is substituted back into Eq. (5), the first term of Eq. (10) would be present in both the numerator and denominator of Eq. (5) and cancel out. Using the similar evaluation for the remaining terms, update Eq. (5) becomes

$$\phi_{efct} \propto \exp\Big(E_{q(\boldsymbol{C}_{-ef},\boldsymbol{T}_{-ef})}\Big(-\log\big(V\eta + N_{\cdot\cdot c\cdot}^{-ef}\big) + \log\big(\eta + N_{\cdot\cdot cv_{ef}}^{-ef}\big) - \log\big(K\alpha + N_{\cdot t\cdot\cdot}^{-ef}\big) + \log\big(\alpha + N_{\cdot tc\cdot}^{-ef}\big)\Big)\Big) \tag{11}$$

for $t' \in \boldsymbol{\tau}_e$ (otherwise ϕ_{efct} is zero), where the first log (·) term in Eq. (11) comes from the first term in Eq. (9), the second log (·) term in Eq. (11) comes from the second term in Eq. (9), and so on.

The log (·) terms in Eq. (10) can be approximated by a second-order Taylor's series expansion about their means (Teh at al. 2006). Consider the Taylor's series expansion of the $\log(b + x)$ function about a particular constant a:

$$\log(b + x) \approx \log(b + a) + \frac{(x - a)}{b + a} - \frac{(x - a)^2}{2(b + a)^2} \tag{12}$$

Applying the expansion in Eq. (12) with $b = V\eta$, $x = N_{\cdot\cdot c\cdot}^{-ef}$, and $a = E_{q(-\boldsymbol{C}_{ef},-\boldsymbol{T}_{ef})}\big(N_{\cdot\cdot c\cdot}^{-ef}\big)$, the first term in Eq. (11) can be approximated as

$$\begin{aligned} & E_{q(\boldsymbol{C}_{-ef},\boldsymbol{T}_{-ef})}\big(-\log\big(V\eta + N_{\cdot\cdot c\cdot}^{-ef}\big)\big) \\ & \overset{(a)}{\approx} -E_q\left(\log\Big(V\eta + E_q\big(N_{\cdot\cdot c\cdot}^{-ef}\big)\Big) + \frac{N_{\cdot\cdot c\cdot}^{-ef} - E_q\big(N_{\cdot\cdot c\cdot}^{-ef}\big)}{V\eta + E_q\big(N_{\cdot\cdot c\cdot}^{-ef}\big)} - \frac{\Big(N_{\cdot\cdot c\cdot}^{-ef} - E_q\big(N_{\cdot\cdot c\cdot}^{-ef}\big)\Big)^2}{2\Big(V\eta + E_q\big(N_{\cdot\cdot c\cdot}^{-ef}\big)\Big)^2}\right) \\ & \overset{(b)}{=} -\log\Big(V\eta + E_q\big(N_{\cdot\cdot c\cdot}^{-ef}\big)\Big) + \frac{Var_q\big(N_{\cdot\cdot c\cdot}^{-ef}\big)}{2\Big(V\eta + E_q\big(N_{\cdot\cdot c\cdot}^{-ef}\big)\Big)^2}, \end{aligned} \tag{13}$$

where the subscript $(\boldsymbol{C}_{-ef}, \boldsymbol{T}_{-ef})$ in $E_{q(\boldsymbol{C}_{-ef},\boldsymbol{T}_{-ef})}(\cdot)$ was omitted in Eq. (13a) to reduce clutter. Eq. (13b) was obtained because the expectation of a constant is itself.

Therefore the first term corresponds to $E_q\left(\log\left(V\eta + E_q\left(N_{\cdot\cdot c\cdot}^{-ef}\right)\right)\right) = \log\left(V\eta + E_q\left(N_{\cdot\cdot c\cdot}^{-ef}\right)\right)$. The second term evaluates to zero because $E_q\left(E_q\left(N_{\cdot\cdot c\cdot}^{-ef}\right)\right) = E_q\left(N_{\cdot\cdot c\cdot}^{-ef}\right)$.

Applying the same approximation for all $\log(\cdot)$ terms in Eq. (11) and rearranging, the update equation for ϕ becomes

$$\phi_{efct} \propto \frac{\left(\eta + E_q\left(N_{\cdot\cdot cv_{ef}}^{-ef}\right)\right)\left(\alpha + E_q\left(N_{\cdot tc\cdot}^{-ef}\right)\right)}{\left(V\eta + E_q\left(N_{\cdot\cdot c\cdot}^{-ef}\right)\right)\left(K\alpha + E_q\left(N_{\cdot t\cdot\cdot}^{-ef}\right)\right)} \tag{14}$$

$$\times\exp\left[\frac{Var_q\left(N_{\cdot\cdot c\cdot}^{-ef}\right)}{2\left(V\eta + E_q\left(N_{\cdot\cdot c\cdot}^{-ef}\right)\right)^2} - \frac{Var_q\left(N_{\cdot\cdot cv_{ef}}^{-ef}\right)}{2\left(\eta + E_q\left(N_{\cdot\cdot cv_{ef}}^{-ef}\right)\right)^2}\right]$$

$$\times\exp\left[\frac{Var_q\left(N_{\cdot t\cdot\cdot}^{-ef}\right)}{2\left(K\alpha + E_q\left(N_{\cdot t\cdot\cdot}^{-ef}\right)\right)^2} - \frac{Var_q\left(N_{\cdot tc\cdot}^{-ef}\right)}{2\left(\alpha + E_q\left(N_{\cdot tc\cdot}^{-ef}\right)\right)^2}\right]$$

The mean and variance of the counts in Eq. (14) can be evaluated using the current estimate of ϕ. For example, $N_{\cdot\cdot c\cdot}^{-ef}$ can be thought of as the number of heads obtained from tossing a coin independently for each focus of each experiment in the entire dataset (excluding the f-th focus of the e-th experiment), where the probability of getting a head for the f'-th activated voxel of the e'-th experiment is equal to $\sum_{t\in\boldsymbol{\tau}_{e'}} \phi_{e'f'ct}$. Thus, the expectation and variance of $N_{\cdot\cdot c\cdot}^{-ef}$ is given by

$$E_q\left(N_{\cdot\cdot c\cdot}^{-ef}\right) = \sum_{e'\neq e, f'\neq f} \sum_{t\in\boldsymbol{\tau}_{e'}} \phi_{e'f'ct}, \tag{15}$$

$$Var_q\left(N_{\cdot\cdot c\cdot}^{-ef}\right) = \sum_{e'\neq e, f'\neq f} \left(\sum_{t\in\boldsymbol{\tau}_{e'}} \phi_{e'f'ct}\right)\left(1 - \sum_{t\in\boldsymbol{\tau}_{e'}} \phi_{e'f'ct}\right).$$

By using the same argument for the remaining terms of Eq. (14), we can evaluate the update equation for ϕ_{efct} given the current estimate of ϕ.

To summarize, the CVB algorithm proceeds by iterating Eq. (14) until convergence. Notice that under CVB inference, the posterior ϕ is estimated without using the point estimates of the model parameters θ and β (unlike the EM algorithm;

see Appendix A3). Given the final estimate of posterior distribution ϕ, the parameters θ and β can be estimated by the posterior means (Teh et al. 2006):

$$\theta_{tc} \propto \quad \alpha + \sum_{e=1}^{E} \sum_{f=1}^{F_e} \phi_{efct} \tag{16}$$

$$\beta_{cv} \propto \quad \eta + \sum_{e=1}^{E} \sum_{f=1}^{F_e} \sum_{t \in \boldsymbol{\tau}_e} \phi_{efct}\, \mathbb{I}(v_{ef} = v), \tag{17}$$

where $\mathbb{I}(v_{ef} = v)$ equals to one if the activation focus v_{ef} corresponds to location v in MNI152 space, and zero otherwise.

A3. Theoretical differences between CVB with Standard Variational Bayes (SVB) and EM algorithm

The CVB algorithm is theoretically better than standard variational Bayes (SVB) inference (Teh et al., 2006). As explained in the previous appendix, CVB algorithm constructs a lower bound to the data log likelihood with respect to the latent variables $(\boldsymbol{C}, \boldsymbol{T})$. On the other hand, the SVB algorithm constructs a lower bound with respect to both latent variables $(\boldsymbol{C}, \boldsymbol{T})$ and model parameters (θ, β). Consequently, CVB provides a tighter lower bound to the data log likelihood:

$$\begin{aligned}
&\log p(\boldsymbol{v} \mid \alpha, \eta, \boldsymbol{\tau}) \\
&\geq E_{q(\boldsymbol{C},\boldsymbol{T})}(\log p(\boldsymbol{v}, \boldsymbol{C}, \boldsymbol{T} \mid \alpha, \eta, \boldsymbol{\tau})) - E_{q(\boldsymbol{C},\boldsymbol{T})}(\log q(\boldsymbol{C}, \boldsymbol{T})) && (18)\\
&\geq E_{q(\boldsymbol{C},\boldsymbol{T})q(\theta,\beta)}(\log p(\boldsymbol{v}, \boldsymbol{C}, \boldsymbol{T}, \theta, \beta \mid \alpha, \eta, \boldsymbol{\tau})) - E_{q(\theta,\beta)}(\log q(\theta, \beta)) && (19)\\
&\qquad - E_{q(\boldsymbol{C},\boldsymbol{T})}(\log q(\boldsymbol{C}, \boldsymbol{T}))
\end{aligned}$$

where the inequality (Eq. (18)) is the same as CVB Eq. (1) and the second inequality (Eq. (19)) corresponds to SVB.

One can also draw parallels between the CVB (Appendix A2) and EM (Yeo et al., 2015) algorithms for the author-topic model. Both algorithms iterate between estimating the posterior distribution of the latent variables $(\boldsymbol{C}, \boldsymbol{T})$ and using the posterior distribution to update the model parameters estimates (θ, β). However, the EM algorithm uses *point* estimates of the model parameters to update the posterior

distribution of $(\boldsymbol{C}, \boldsymbol{T})$. In contrast, the CVB algorithm avoids doing so (Eq. (14)) and might therefore produce better estimates of the parameters (Ngo et al. 2016).

In practice, we find the CVB algorithm to be less sensitive than the EM algorithm to the initialization of the hyperparameters α and η. This is not an issue for a big dataset (e.g., BrainMap; Yeo et al., 2015) because the data will overwhelm the priors. However, this issue is important for small datasets like those utilized in this work. For the CVB algorithm, the hyperparameters α and η were set to 100 and 0.01 respectively across all of our experiments. Perturbing α and η by two orders of magnitude did not significantly change the model parameters estimated by CVB algorithm, suggesting its robustness. This was not the case for the EM algorithm.

A4. Estimating Number of Components using Bayesian Information Criterion (BIC)

Bayesian Information Criterion (BIC) is commonly used for model selection in machine learning (Schwarz, 1978). BIC favors models that best fit the data, while also penalizing models with more parameters. The BIC for the author-topic model is given by:

$$BIC = \log p(\boldsymbol{v} \mid \theta, \beta, \boldsymbol{\tau}) - \frac{1}{2}\left(k_\theta + k_\beta\right) \log|\boldsymbol{v}| \tag{20}$$

$$= \sum_{e=1}^{E} \log \frac{1}{|\boldsymbol{\tau}_e|} \sum_{f=1}^{F_e} \sum_{c=1}^{K} \sum_{t \in \boldsymbol{\tau}_e} \beta_{c v_{ef}} \theta_{tc} - \frac{1}{2}\left(k_\theta + k_\beta\right) \log \sum_{e=1}^{E} |\boldsymbol{v}_e| \tag{21}$$

where the first term is the log likelihood of the activation foci $\boldsymbol{v}$ given the model parameters estimates θ and β, and the second term is the penalty based on the number of model parameters. $|\boldsymbol{v}_e|$ and $|\boldsymbol{\tau}_e|$ are the number of foci and tasks employed in the e-th experiment. k_θ and k_β are the number of free model parameters. k_θ is the number of free parameters in the $M \times K$ matrix θ, which is equal to $M \times (K-1)$ since each row sums to one. k_β is the approximated number of independent elements in the $K \times V$ matrix β. Each row of β can be interpreted as a spatially smoothed brain image (see Appendix A5). Therefore we approximated the number of independent elements in each row of β by the number of resolution elements (resels) in the corresponding brain image (Worsley et al. 1992) using AFNI (Cox 1996).

Models with a higher number of components K fit the data better, resulting in a higher data log likelihood (first term of Eq. (20)). On the other hand, a higher K also increases the number of free parameters $(k_\theta + k_\beta)$, which results in a higher penalty (second term of Eq. (20)). A higher BIC values indicates a better model.

A5. Implementation details

Each experimental contrast reported a set of coordinates of statistically significant local maxima in the activation images. The spatial locations of the activation foci were reported in or transformed to the MNI152 coordinate system (Lancaster et al., 2007). Using standard meta-analysis procedure (Wager et al. 2007; Yarkoni et al. 2011; Yeo et al. 2015), a 2-mm-resolution binary activation image was created for each experimental contrast, in which a voxel was given a value of 1 if it was within 10mm of any activation focus, and 0 otherwise. Thus, the set of F_e activated voxels of the e-th experiment in the author-topic model corresponds to the set of voxels with a value of 1 in the corresponding 2-mm-resolution binary activation image.

The model's hyperparameters were set to be $\alpha = 100$ and $\eta = 0.01$ across all experiments. Perturbing α and η by two orders of magnitude did not significantly change the results. The posterior distribution ϕ was randomly initialized. The CVB algorithm then updated the posterior distribution ϕ (Eq. (14)) until convergence. Given the estimate of ϕ, CVB algorithm then computed the model parameters θ and β (Eq. (16) and Eq. (17)). For a given number of components K, the procedure was repeated with 100 random initializations resulting in 100 estimates. The estimate resulting in the maximum lower bound of the data log likelihood (Eq. (1)) was taken as the final estimate.

We repeated the procedure with for different number of cognitive components K. BIC was computed for each value of K (Appendix A4). Higher BIC implied better model parameters estimates. The model parameters with the highest BIC were presented in the Results and Discussion sections.

A6. Approximation of Pr(co-activation pattern | task)

For the co-activation analysis of IFJ, each experiment was treated as its own unique task. To help interpret the co-activation pattern in terms of BrainMap task

categories (also known as paradigm classes), we estimated the the probability of the c-th co-activation pattern being utilized by the t-th task posthoc:

$$\Pr(co - activation\ c \mid task\ t) \propto \sum_{e=1}^{E} \frac{\theta_{ec} \mathbb{I}(t \in \boldsymbol{\tau}_e)}{|\boldsymbol{\tau}_e|}, \tag{22}$$

where θ_{ec} was the estimated probability that the e-th experiment would recruit the c-th co-activation pattern, $\boldsymbol{\tau}_e$ was the set of tasks utilized in the e-th experiment, and $\mathbb{I}(t \in \boldsymbol{\tau}_e)$ is an indicator function that was equal to 1 if the t-th task was one of the collection of tasks $\boldsymbol{\tau}_e$ utilized by the e-th experiment and 0 otherwise. Eq. (22) can be interpreted as weighted average of θ_{ec} across all experiments utilizing task t with the weight being smaller if an experiment utilizes many tasks. For example, if the 3rd experiment utilized “n-back” and “Stroop” tasks, the probability contributed by this experiment to the computation of the probability of “n-back” recruiting co-activation pattern C1 ($\Pr(co - activation\ C1 \mid "n - back")$) would be the probability of the experiment recruiting co-activation pattern C1 (i.e., θ_{31}), divided by the number of tasks, which is two.

References

Andrews-Hanna JR, Reidler JS, Huang C, Buckner RL. 2010. Evidence for the default networks role in spontaneous cognition. Journal of Neurophysiology. 104:322-335.

Andrews-Hanna JR, Reidler JS, Sepulcre J, Poulin R, Buckner RL. 2010. Functional-anatomic fractionation of the brains default network. Neuron. 65:550-562.

Andrews-Hanna JR, Smallwood J, Spreng, RN. 2014. The default network and self-generated thought: component processes, dynamic control, and clinical relevance. Annals of the New York Academy of Sciences. 1316:29-52.

Andrews-Hanna JR. 2012. The brain's default network and its adaptive role in internal mentation. The Neuroscientist. 18:251-270.

Asplund CL, Todd JJ, Snyder AP, Marois R. 2010. A central role for the lateral prefrontal cortex in goal-directed and stimulus-driven attention. Nature Neuroscience. 13:507-512.

Atance CM, O'Neill DK. 2001. Episodic future thinking. Trends in Cognitive Sciences. 5:533-539.

Baird B, Smallwood J, Schooler JW. 2011. Back to the future: autobiographical planning and the functionality of mind-wandering. Consciousness and Cognition. 20:1604-1611.

Baldauf D, Desimone R. 2014. Neural mechanisms of object-based attention. Science. 344:424-427.

Barch DM, Braver TS, Akbudak E, Conturo T, Ollinger J, Snyder A. 2001. Anterior cingulate cortex and response conflict: effects of response modality and processing domain. Cerebral Cortex. 11:837-848.

Barrett LF, Satpute AB. 2013. Large-scale brain networks in affective and social neuroscience: Towards an integrative functional architecture of the brain. Current Opinion in Neurobiology. 23:361-372.

Beal MJ. 2003. Variational algorithms for approximate Bayesian inference, University of London United Kingdom.

Beissner F, Meissner K, Bär KJ, Napadow V. 2013. The autonomic brain: an activation likelihood estimation meta-analysis for central processing of autonomic function. Journal of Neuroscience. 33:10503-10511.

Berman KF, Ostrem JL, Randolph C, Gold J, Goldberg TE, Coppola R, Carson RE, Herscovitch P, Weinberger DR. 1995. Physiological activation of a cortical network during performance of the Wisconsin Card Sorting Test: a positron emission tomography study. Neuropsychologia. 33:1027-1046.

Bertolero MA, Yeo BTT, D'Esposito M. 2015. The modular and integrative functional architecture of the human brain. Proceedings of the National Academy of Sciences. 112:E6798-E6807.

Binder JR, Desai RH, Graves WW, Conant LL. 2009. Where is the semantic system? A critical review and meta-analysis of 120 functional neuroimaging studies. Cerebral Cortex. 19:2767-2796.

Binder JR, Desai RH. 2011. The neurobiology of semantic memory. Trends in Cognitive Sciences. 15:527-536.

Brass M, Derrfuss J, Forstmann B, von Cramon DY. 2005. The role of the inferior frontal junction area in cognitive control. Trends in Cognitive Sciences. 9:314-316.

Brass M, von Cramon DY. 2002. The role of the frontal cortex in task preparation. Cerebral Cortex. 12:908-914.

Braver TS, Barch DM, Gray JR, Molfese DL, Snyder A. 2001. Anterior cingulate cortex and response conflict: effects of frequency, inhibition and errors. Cerebral Cortex. 11:825-836.
Brown AD, Addis DR, Romano TA, Marmar CR, Bryant RA, Hirst W, Schacter DL. 2014. Episodic and semantic components of autobiographical memories and imagined future events in post-traumatic stress disorder. Memory. 22:595-604.
Buckner RL, Andrews-Hanna JR, Schacter DL. 2008. The brains default network. Annals of the New York Academy of Sciences. 1124:1-38.
Buckner RL, Carroll DC. 2007. Self-projection and the brain. Trends in Cognitive Sciences. 11:49-57.
Buckner RL, Krienen FM, Castellanos A, Diaz JC, Yeo BTT. 2011. The organization of the human cerebellum estimated by intrinsic functional connectivity. Journal of Neurophysiology. 106:2322-2345.
Burgess N, Maguire EA, OKeefe J. 2002. The human hippocampus and spatial and episodic memory. Neuron. 35:625-641.
Button KS, Ioannidis JP, Mokrysz C, Nosek BA, Flint J, Robinson ES, Munafò MR. 2013. Power failure: why small sample size undermines the reliability of neuroscience. Nature Reviews. Neuroscience. 14:365.
Byrne P, Becker S, Burgess N. 2007. Remembering the past and imagining the future: a neural model of spatial memory and imagery. Psychological Review. 114:340.
Bzdok D, Langner R, Schilbach L, Engemann DA, Laird AR, Fox PT, Eickhoff S. 2013. Segregation of the human medial prefrontal cortex in social cognition. Frontiers in Human Neuroscience. 7:232.
Callard F, Margulies DS. 2014. What we talk about when we talk about the default mode network. Frontiers in human neuroscience. 8:619.
Carp J. 2012. The secret lives of experiments: methods reporting in the fMRI literature. Neuroimage. 63:289-300.
Cauda F, Costa T, Torta DME, Sacco K, Dagata F, Duca S, Geminiani G, Fox PT, Vercelli A. 2012. Meta-analytic clustering of the insular cortex: characterizing the meta-analytic connectivity of the insula when involved in active tasks. Neuroimage. 62:343-355.
Chein JM, Fissell K, Jacobs S, Fiez JA. 2002. Functional heterogeneity within Brocas area during verbal working memory. Physiology, Behavior. 77:635-639.
Chikazoe J, Jimura K, Asari T, Yamashita K, Morimoto H, Hirose S, Miyashita Y, Konishi S. 2009. Functional dissociation in right inferior frontal cortex during performance of go/no-go task. Cerebral Cortex. 19:146-152.
Chikazoe J, Jimura K, Hirose S, Yamashita K, Miyashita Y, Konishi S. 2009. Preparation to inhibit a response complements response inhibition during performance of a stop-signal task. Journal of Neuroscience. 29:15870-15877.
Christoff K, Irving ZC, Fox KCR, Spreng RN, Andrews-Hanna JR. 2016. Mind-wandering as spontaneous thought: A dynamic framework. Nature Reviews Neuroscience. 17:718–731.
Clos M, Rottschy C, Laird AR, Fox PT, Eickhoff SB. 2014. Comparison of structural covariance with functional connectivity approaches exemplified by an investigation of the left anterior insula. NeuroImage. 99:269-280.
Cortese S, Kelly C, Chabernaud C, Proal E, Di Martino A, Milham MP, Castellanos FX. 2012. Toward systems neuroscience of ADHD: a meta-analysis of 55 fMRI studies. American Journal of Psychiatry. 169:1038-1055.
Costafreda SG, Brammer MJ, David AS, Fu CHY. 2008. Predictors of amygdala activation during the processing of emotional stimuli: a meta-analysis of 385

PET and fMRI studies. Brain Research Reviews. 58:57-70.
Cox RW. 1996. AFNI: software for analysis and visualization of functional magnetic resonance neuroimages. Computers and Biomedical research. 29:162-173.
Crossley NA, Mechelli A, Scott J, Carletti F, Fox PT, McGuire P, Bullmore ET. 2014. The hubs of the human connectome are generally implicated in the anatomy of brain disorders. Brain. 137:2382-2395.
David SP, Ware JJ, Chu IM, Loftus PD, Fusar-Poli P, Radua J, Munafт MR, Ioannidis JPA. 2013. Potential reporting bias in fMRI studies of the brain. PloS one. 8:e70104.
Decety J, Lamm C. 2007. The role of the right temporoparietal junction in social interaction: how low-level computational processes contribute to meta-cognition. The Neuroscientist. 13:580-593.
Delaveau P, Jabourian M, Lemogne C, Guionnet S, Bergouignan L, Fossati P. 2011. Brain effects of antidepressants in major depression: a meta-analysis of emotional processing studies. Journal of Affective Disorders. 130:66-74.
Derrfuss J, Brass M, Neumann J, von Cramon DY. 2005. Involvement of the inferior frontal junction in cognitive control: Meta-analyses of switching and Stroop studies. Human Brain Mapping. 25:22-34.
Derrfuss J, Brass M, Von Cramon DY. 2004. Cognitive control in the posterior frontolateral cortex: evidence from common activations in task coordination, interference control, and working memory. Neuroimage. 23:604-612.
Di Martino A, Ross K, Uddin LQ, Sklar AB, Castellanos FX, Milham MP. 2009. Functional brain correlates of social and nonsocial processes in autism spectrum disorders: an activation likelihood estimation meta-analysis. Biological Psychiatry. 65:63-74.
Duncan J. 2010. The multiple-demand (MD) system of the primate brain: mental programs for intelligent behaviour. Trends in cognitive sciences. 14:172-179.
Duncan J. 2013. The structure of cognition: attentional episodes in mind and brain. Neuron. 80:35-50.
Eickhoff SB, Bzdok D, Laird AR, Kurth F, Fox PT. 2012. Activation likelihood estimation meta-analysis revisited. Neuroimage. 59:2349-2361.
Eickhoff SB, Jbabdi S, Caspers S, Laird AR, Fox PT, Zilles K, Behrens TEJ. 2010. Anatomical and functional connectivity of cytoarchitectonic areas within the human parietal operculum. Journal of Neuroscience. 30:6409-6421.
Eickhoff SB, Laird AR, Grefkes C, Wang LE, Zilles K, Fox PT. 2009. Coordinate-based activation likelihood estimation meta-analysis of neuroimaging data: A random-effects approach based on empirical estimates of spatial uncertainty. Human Brain Mapping. 30:2907-2926.
Fedorenko E, Duncan J, Kanwisher N. 2013. Broad domain generality in focal regions of frontal and parietal cortex. Proceedings of the National Academy of Sciences. 110:16616-16621.
Fischl B. 2012. FreeSurfer. Neuroimage. 62:774-781.
Fitzgerald PB, Laird AR, Maller J, Daskalakis ZJ. 2008. A meta-analytic study of changes in brain activation in depression. Human Brain Mapping. 29:683-695.
Fox PT, Lancaster JL, Laird AR, Eickhoff SB. 2014. Meta-analysis in human neuroimaging: computational modeling of large-scale databases. Annual Review of Neuroscience. 37:409-434.
Fox PT, Lancaster JL. 2002. Mapping context and content: the BrainMap model. Nature Reviews Neuroscience. 3:319-321.
Friederici AD. 2002. Towards a neural basis of auditory sentence processing. Trends

in Cognitive Sciences. 6:78-84.
Frith C, Frith U. 2005. Theory of mind. Current Biology. 15:R644-R645.
Frith U, Frith CD. 2003. Development and neurophysiology of mentalizing. Philosophical Transactions of the Royal Society B: Biological Sciences. 358:459-473.
Gernsbacher MA, Hallada BM, Robertson RRW. 1998. How automatically do readers infer fictional characters emotional states?. Scientific Studies of Reading. 2:271-300.
Glahn DC, Ragland JD, Abramoff A, Barrett J, Laird AR, Bearden CE, Velligan DI. 2005. Beyond hypofrontality: A quantitative meta-analysis of functional neuroimaging studies of working memory in schizophrenia. Human Brain Mapping. 25:60-69.
Gorgolewski KJ, Lurie D, Urchs S, Kipping JA, Craddock RC, Milham MP, Margulies DS, Smallwood J. 2014. A correspondence between individual differences in the brain's intrinsic functional architecture and the content and form of self-generated thoughts. PloS one. 9:e97176.
Guajardo NR, Watson AC. 2002. Narrative discourse and theory of mind development. The Journal of Genetic Psychology. 163:305-325.
Hassabis D, Kumaran D, Vann SD, Maguire EA. 2007. Patients with hippocampal amnesia cannot imagine new experiences. Proceedings of the National Academy of Sciences. 104:1726-1731.
Hassabis D, Maguire EA. 2007. Deconstructing episodic memory with construction. Trends in Cognitive Sciences. 11:299-306.
Humphreys GF, Hoffman P, Visser M, Binney RJ, Ralph MAL. 2015. Establishing task-and modality-dependent dissociations between the semantic and default mode networks. Proceedings of the National Academy of Sciences. 112:7857-7862.
Irish M, Addis DR, Hodges JR, Piguet O. 2012. Considering the role of semantic memory in episodic future thinking: evidence from semantic dementia. Brain. 135:2178-2191.
Jobard G, Vigneau M, Mazoyer B, Tzourio-Mazoyer N. 2007. Impact of modality and linguistic complexity during reading and listening tasks. Neuroimage. 34:784-800.
Kim C, Johnson NF, Cilles SE, Gold BT. 2011. Common and distinct mechanisms of cognitive flexibility in prefrontal cortex. Journal of Neuroscience. 31:4771-4779.
Kim H. 2012. A dual-subsystem model of the brains default network: self-referential processing, memory retrieval processes, and autobiographical memory retrieval. Neuroimage. 61:966-977.
Knutson B, Wimmer GE, Rick S, Hollon NG, Prelec D, Loewenstein G. 2008. Neural antecedents of the endowment effect. Neuron. 58:814-822.
Konishi S, Hayashi T, Uchida I, Kikyo H, Takahashi E, Miyashita Y. 2002. Hemispheric asymmetry in human lateral prefrontal cortex during cognitive set shifting. Proceedings of the National Academy of Sciences. 99:7803-7808.
Konishi S, Jimura K, Asari T, Miyashita Y. 2003. Transient activation of superior prefrontal cortex during inhibition of cognitive set. Journal of Neuroscience. 23:7776-7782.
Konishi S, Nakajima K, Uchida I, Kameyama M, Nakahara K, Sekihara K, Miyashita Y. 1998. Transient activation of inferior prefrontal cortex during cognitive set shifting. Nature Neuroscience. 1:80-84.
Koski L, Paus T. 2000. Functional connectivity of the anterior cingulate cortex within

the human frontal lobe: a brain-mapping meta-analysis. Executive Control and the Frontal Lobe: Current Issues. 55-65.
Kühn S, Gallinat J. 2013. Resting-state brain activity in schizophrenia and major depression: a quantitative meta-analysis. Schizophrenia Bulletin. 39:358-365.
Laird AR, Eickhoff SB, Li K, Robin DA, Glahn DC, Fox PT. 2009. Investigating the functional heterogeneity of the default mode network using coordinate-based meta-analytic modeling. Journal of Neuroscience. 29:14496-14505.
Laird AR, Eickhoff SB, Kurth F, Fox PM, Uecker AM, Turner JA, Robinson JL, Lancaster JL, Fox PT. 2009. ALE meta-analysis workflows via the Brainmap database: progress towards a probabilistic functional brain atlas. Frontiers in neuroinformatics. 3:23.
Laird AR, Fox PM, Eickhoff SB, Turner JA, Ray KL, McKay DR, Glahn DC, Beckmann CF, Smith SM, Fox PT. 2011. Behavioral interpretations of intrinsic connectivity networks. Journal of Cognitive Neuroscience. 23:4022-4037.
Laird AR, Fox PM, Price CJ, Glahn DC, Uecker AM, Lancaster JL, Turkeltaub PE, Kochunov P, Fox PT. 2005. ALE meta-analysis: Controlling the false discovery rate and performing statistical contrasts. Human brain mapping. 25:155-164.
Lancaster JL, Tordesillas-Gutiérrez D, Martinez M, Salinas F, Evans A, Zilles K, Mazziotta JC, Fox PT. 2007. Bias between MNI and Talairach coordinates analyzed using the ICBM-152 brain template. Human Brain Mapping. 28:1194-1205.
Leslie AM. 1987. Pretense and representation: The origins of "theory of mind". Psychological Review. 94:412.
Levy BJ, Wagner AD. 2011. Cognitive control and right ventrolateral prefrontal cortex: reflexive reorienting, motor inhibition, and action updating. Annals of the New York Academy of Sciences. 1224:40-62.
Mar RA. 2011. The neural bases of social cognition and story comprehension. Annual Review of Psychology. 62:103-134.
Mason RA, Williams DL, Kana RK, Minshew N, Just MA. 2008. Theory of mind disruption and recruitment of the right hemisphere during narrative comprehension in autism. Neuropsychologia. 46:269-280.
Mason RA, Williams DL, Kana RK, Minshew N, Just MA. 2008. Theory of mind disruption and recruitment of the right hemisphere during narrative comprehension in autism. Neuropsychologia. 46:269-280.
Mayer JS, Roebroeck A, Maurer K, Linden DEJ. 2010. Specialization in the default mode: Task-induced brain deactivations dissociate between visual working memory and attention. Human Brain Mapping. 31:126-139.
Mesulam M. 1990. Large-scale neurocognitive networks and distributed processing for attention, language, and memory. Annals of Neurology. 28:597-613.
Minzenberg MJ, Laird AR, Thelen S, Carter CS, Glahn DC. 2009. Meta-analysis of 41 functional neuroimaging studies of executive function in schizophrenia. Archives of General Psychiatry. 66:811-822.
Moscovitch M, Cabeza R, Winocur G, Nadel L. 2016. Episodic Memory and Beyond: The Hippocampus and Neocortex in Transformation. Annual Review of Psychology. 67:105-134.
Muhle-Karbe PS, Derrfuss J, Lynn MT, Neubert FX, Fox PT, Brass M, Eickhoff SB. 2015. Co-activation-based parcellation of the lateral prefrontal cortex delineates the inferior frontal junction area. Cerebral Cortex. 26:2225-2241.
Müller VI, Cieslik EC, Serbanescu I, Laird AR, Fox PT, Eickhoff SB. 2017. Altered brain activity in unipolar depression revisited: meta-analyses of neuroimaging

studies. JAMA psychiatry. 74:47-55.
Ngo GH, Eickhoff SB, Fox PT, Yeo BTT. 2016. Collapsed variational Bayesian inference of the author-topic model: application to large-scale coordinate-based meta-analysis. Proceedings of the 2016 International Workshop in Pattern Recognition in Neuroimaging (PRNI).
Nickl-Jockschat T, Janouschek H, Eickhoff SB, Eickhoff CR. 2015. Lack of meta-analytic evidence for an impact of COMT Val158Met genotype on brain activation during working memory tasks. Biological Psychiatry. 78:e43-e46
Omori M, Yamada H, Murata T, Sadato N, Tanaka M, Ishii Y, Isaki K, Yonekura Y. 1999. Neuronal substrates participating in attentional set-shifting of rules for visually guided motor selection: a functional magnetic resonance imaging investigation. Neuroscience Research. 33:317-323.
Pardo JV, Pardo PJ, Janer KW, Raichle ME. 1990. The anterior cingulate cortex mediates processing selection in the Stroop attentional conflict paradigm. Proceedings of the National Academy of Sciences. 87:256-259.
Pesenti M, Thioux M, Seron X, De Volder A. 2000. Neuroanatomical substrates of Arabic number processing, numerical comparison, and simple addition: A PET study. Journal of Cognitive Neuroscience. 12:461-479.
Peters J, Büchel C. 2010. Episodic future thinking reduces reward delay discounting through an enhancement of prefrontal-mediotemporal interactions. Neuron. 66:138-148.
Philip RCM, Dauvermann MR, Whalley HC, Baynham K, Lawrie SM, Stanfield AC. 2012. A systematic review and meta-analysis of the fMRI investigation of autism spectrum disorders. Neuroscience, Biobehavioral Reviews. 36:901-942.
Poeppel D, Guillemin A, Thompson J, Fritz J, Bavelier D, Braun AR. 2004. Auditory lexical decision, categorical perception, and FM direction discrimination differentially engage left and right auditory cortex. Neuropsychologia. 42:183-200.
Poldrack RA, Mumford JA, Schonberg T, Kalar D, Barman B, Yarkoni T. 2012. Discovering relations between mind, brain, and mental disorders using topic mapping. PLoS Comput Biol. 8:e1002707.
Poldrack RA, Wagner AD, Prull MW, Desmond JE, Glover GH, Gabrieli JDE. 1999. Functional specialization for semantic and phonological processing in the left inferior prefrontal cortex. Neuroimage. 10:15-35.
Poldrack RA, Yarkoni T. 2016. From brain maps to cognitive ontologies: informatics and the search for mental structure. Annual Review of Psychology. 67:587-612.
Poldrack RA. 2006. Can cognitive processes be inferred from neuroimaging data?. Trends in Cognitive Sciences. 10:59-63.
Poline J, Breeze JL, Ghosh SS, Gorgolewski K, Halchenko YO, Hanke M, Helmer KG, Marcus DS, Poldrack RA, Schwartz Y, others. 2012. Data sharing in neuroimaging research. Frontiers in Neuroinformatics. 6:9.
Pompei F, Jogia J, Tatarelli R, Girardi P, Rubia K, Kumari V, Frangou S. 2011. Familial and disease specific abnormalities in the neural correlates of the Stroop Task in Bipolar Disorder. Neuroimage. 56:1677-1684.
Prebble SC, Addis DR, Tippett LJ. 2013. Autobiographical memory and sense of self.. Psychological bulletin. 139:815.
Race E, Keane MM, Verfaellie M. 2011. Medial temporal lobe damage causes deficits in episodic memory and episodic future thinking not attributable to deficits in narrative construction. Journal of Neuroscience. 31:10262-10269.
Ragland JD, Laird AR, Ranganath C, Blumenfeld RS, Gonzales SM, Glahn DC.

2009. Prefrontal activation deficits during episodic memory in schizophrenia. American Journal of Psychiatry. 166:863-874.
Raichle ME, MacLeod AM, Snyder AZ, Powers WJ, Gusnard DA, Shulman GL. 2001. A default mode of brain function. Proceedings of the National Academy of Sciences. 98:676-682.
Reid AT, Bzdok D, Genon S, Langner R, Müller VI, Eickhoff CR, Hoffstaedter F, Cieslik, E.-C.; Fox PT, Laird AR, others. 2016. ANIMA: A data-sharing initiative for neuroimaging meta-analyses. Neuroimage. 124:1245-1253.
Reid AT, Bzdok D, Langner R, Fox PT, Laird AR, Amunts K, Eickhoff SB, Eickhoff CR. 2016. Multimodal connectivity mapping of the human left anterior and posterior lateral prefrontal cortex. Brain Structure and Function. 221:2589-2605.
Robinson JL, Laird AR, Glahn DC, Lovallo WR, Fox PT. 2010. Metaanalytic connectivity modeling: delineating the functional connectivity of the human amygdala. Human Brain Mapping. 31:173-184.
Rosen-Zvi M, Chemudugunta C, Griffiths T, Smyth P, Steyvers M. 2010. Learning author-topic models from text corpora. ACM Transactions on Information Systems (TOIS). 28:4.
Rosenbaum RS, Gilboa A, Levine B, Winocur G, Moscovitch M. 2009. Amnesia as an impairment of detail generation and binding: evidence from personal, fictional, and semantic narratives in KC. Neuropsychologia. 47:2181-2187.
Rosenbaum RS, Stuss DT, Levine B, Tulving E. 2007. Theory of mind is independent of episodic memory. Science. 318:1257-1257.
Rottschy C, Langner R, Dogan I, Reetz K, Laird AR, Schulz JB, Fox PT, Eickhoff SB. 2012. Modelling neural correlates of working memory: a coordinate-based meta-analysis. Neuroimage. 60:830-846.
Salomon R, Levy DR, Malach R. 2014. Deconstructing the default: Cortical subdivision of the default mode/intrinsic system during self-related processing. Human Brain Mapping. 35:1491-1502.
Schacter DL, Addis DR, Buckner RL. 2007. Remembering the past to imagine the future: the prospective brain. Nature Reviews Neuroscience. 8:657-661.
Schwarz G, others. 1978. Estimating the dimension of a model. The Annals of Statistics. 6:461-464.
Seghier ML, Price CJ. 2012. Functional heterogeneity within the default network during semantic processing and speech production. Frontiers in Psychology. 3:281.
Sestieri C, Corbetta M, Romani GL, Shulman GL. 2011. Episodic memory retrieval, parietal cortex, and the default mode network: functional and topographic analyses. Journal of Neuroscience. 31:4407-4420.
Sevinc G, Spreng RN. 2014. Contextual and perceptual brain processes underlying moral cognition: a quantitative meta-analysis of moral reasoning and moral emotions. PloS one. 9:e87427.
Shackman AJ, Salomons TV, Slagter HA, Fox AS, Winter JJ, Davidson RJ. 2011. The integration of negative affect, pain and cognitive control in the cingulate cortex. Nature Reviews Neuroscience. 12:154-167.
Shulman GL, Fiez JA, Corbetta M, Buckner RL, Miezin FM, Raichle ME, Petersen SE. 1997. Common blood flow changes across visual tasks: II. Decreases in cerebral cortex. Journal of Cognitive Neuroscience. 9:648-663.
Simões-Franklin C, Hester R, Shpaner M, Foxe JJ, Garavan H. 2010. Executive function and error detection: the effect of motivation on cingulate and ventral striatum activity. Human Brain Mapping. 31:458-469.

Slaughter V, Peterson CC, Mackintosh E. 2007. Mind what mother says: Narrative input and theory of mind in typical children and those on the autism spectrum. Child Development. 78:839-858.
Small GW, Moody TD, Siddarth P, Bookheimer SY. 2009. Your brain on Google: patterns of cerebral activation during internet searching. The American Journal of Geriatric Psychiatry. 17:116-126.
Smallwood J. 2013. Distinguishing how from why the mind wanders: a process–occurrence framework for self-generated mental activity. Psychological Bulletin. 139:519
Smallwood J, Schooler JW, Turk DJ, Cunningham SJ, Burns P, Macrae CN. 2011. Self-reflection and the temporal focus of the wandering mind. Consciousness and Cognition. 20:1120-1126.
Smith SM, Fox PT, Miller KL, Glahn DC, Fox PM, Mackay CE, Filippini N, Watkins KE, Toro R, Laird AR, others. 2009. Correspondence of the brains functional architecture during activation and rest. Proceedings of the National Academy of Sciences. 106:13040-13045.
Sneve MH, Magnussen S, Alnæs D, Endestad T, D'Esposito M. 2013. Top-down modulation from inferior frontal junction to FEFs and intraparietal sulcus during short-term memory for visual features. Journal of Cognitive Neuroscience. 25:1944-1956.
Spaniol J, Davidson PSR, Kim ASN, Han H, Moscovitch M, Grady CL. 2009. Event-related fMRI studies of episodic encoding and retrieval: meta-analyses using activation likelihood estimation. Neuropsychologia. 47:1765-1779.
Spreng RN, Mar RA, Kim ASN. 2009. The common neural basis of autobiographical memory, prospection, navigation, theory of mind, and the default mode: a quantitative meta-analysis. Journal of Cognitive Neuroscience. 21:489-510.
Spreng RN, Andrews-Hanna JR. 2015. The default network and social cognition. Brain Mapping: An Encyclopedic Reference. 165-169
Sylvester CC, Wager TD, Lacey SC, Hernandez L, Nichols TE, Smith EE, Jonides J. 2003. Switching attention and resolving interference: fMRI measures of executive functions. Neuropsychologia. 41:357-370.
Teh YW, Newman D, Welling M. 2006. A collapsed variational Bayesian inference algorithm for latent Dirichlet allocation. NIPS. 6:1378-1385.
Toro R, Fox PT, Paus T. 2008. Functional coactivation map of the human brain. Cerebral Cortex. 18:2553-2559.
Turkeltaub PE, Eden GF, Jones KM, Zeffiro TA. 2002. Meta-analysis of the functional neuroanatomy of single-word reading: method and validation. Neuroimage. 16:765-780.
Turkeltaub PE, Eickhoff SB, Laird AR, Fox M, Wiener M, Fox P. 2012. Minimizing within-experiment and within-group effects in activation likelihood estimation meta-analyses. Human Brain Mapping. 33:1-13.
Tyler LK, Stamatakis EA, Post B, Randall B, Marslen-Wilson W. 2005. Temporal and frontal systems in speech comprehension: an fMRI study of past tense processing. Neuropsychologia. 43:1963-1974.
Uddin LQ, Clare Kelly AM, Biswal BB, Xavier Castellanos F, Milham MP. 2009. Functional connectivity of default mode network components: correlation, anticorrelation, and causality. Human Brain Mapping. 30:625-637.
Van Essen DC, Smith SM, Barch DM, Behrens TEJ, Yacoub E, Ugurbil K, Consortium, WU-Minn HCP Consortium, others. 2013. The WU-Minn human connectome project: an overview. Neuroimage. 80:62-79.

Van Overwalle F. 2009. Social cognition and the brain: a meta-analysis. Human Brain Mapping. 30:829-858.
Wager TD, Lindquist M, Kaplan L. 2007. Meta-analysis of functional neuroimaging data: current and future directions. Social Cognitive and Affective Neuroscience. 2:150-158.
Wager TD, Lindquist MA, Nichols TE, Kober H, Van Snellenberg JX. 2009. Evaluating the consistency and specificity of neuroimaging data using meta-analysis. Neuroimage. 45:S210-S221.
Wager TD, Phan KL, Liberzon I, Taylor SF. 2003. Valence, gender, and lateralization of functional brain anatomy in emotion: a meta-analysis of findings from neuroimaging. Neuroimage. 19:513-531.
Wagner AD, Paré-Blagoev EJ, Clark J, Poldrack RA. 2001. Recovering meaning: left prefrontal cortex guides controlled semantic retrieval. Neuron. 31:329-338.
Wagner RK, Torgesen JK. 1987. The nature of phonological processing and its causal role in the acquisition of reading skills. Psychological bulletin. 101:192.
Weiss EM, Golaszewski S, Mottaghy FM, Hofer A, Hausmann A, Kemmler G, Kremser C, Brinkhoff C, Felber SR, Fleischhacker WW. 2003. Brain activation patterns during a selective attention test – a functional MRI study in healthy volunteers and patients with schizophrenia. Psychiatry Research: Neuroimaging. 123:1-15.
Worsley KJ, Marrett S, Neelin P, Vandal AC, Friston KJ, Evans AC, others. 1996. A unified statistical approach for determining significant signals in images of cerebral activation. Human Brain Mapping. 4:58-73.
Xu B, Grafman J, Gaillard WD, Ishii K, Vega-Bermudez F, Pietrini P, Reeves-Tyer P, DiCamillo P, Theodore W. 2001. Conjoint and extended neural networks for the computation of speech codes: the neural basis of selective impairment in reading words and pseudowords. Cerebral Cortex. 11:267-277.
Xue G, Ghahremani DG, Poldrack RA. 2008. Neural substrates for reversing stimulus–outcome and stimulus–response associations. Journal of Neuroscience. 28:11196-11204.
Yarkoni T, Poldrack RA, Nichols TE, Van Essen DC, Wager TD. 2011. Large-scale automated synthesis of human functional neuroimaging data. Nature Methods. 8:665-670.
Yeo BTT, Krienen FM, Chee MWL, Buckner RL. 2014. Estimates of segregation and overlap of functional connectivity networks in the human cerebral cortex. Neuroimage. 88:212-227.
Yeo BTT, Krienen FM, Eickhoff SB, Yaakub SN, Fox PT, Buckner RL, Asplund CL, Chee MWL. 2015. Functional specialization and flexibility in human association cortex. Cerebral Cortex. 25:3654-3672.
Zago L, Pesenti M, Mellet E, Crivello F, Mazoyer B, Tzourio-Mazoyer N. 2001. Neural correlates of simple and complex mental calculation. Neuroimage. 13.
Zald DH, McHugo M, Ray KL, Glahn DC, Eickhoff SB, Laird AR. 2014. Meta-analytic connectivity modeling reveals differential functional connectivity of the medial and lateral orbitofrontal cortex. Cerebral Cortex. 24:232-248.
Zandbelt BB, van Buuren M, Kahn RS, Vink M. 2011. Reduced proactive inhibition in schizophrenia is related to corticostriatal dysfunction and poor working memory. Biological Psychiatry. 70:1151-1158.
Zanto TP, Rubens MT, Bollinger J, Gazzaley A. 2010. Top-down modulation of visual feature processing: the role of the inferior frontal junction. Neuroimage. 53:736-745.

Table S1: Definitions of 26 BrainMap paradigm classes tagged to experiments activating the IFJ. Only paradigm classes tagged to at least 5 experiments were included. The definitions were extracted from BrainMap lexicon, available at http://www.brainmap.org/scribe/BrainMapLex.xls

Paradigm Class	Definition
Counting/Calculation	Count, add, subtract, multiply, or divide various stimuli (numbers, bars, dots, etc.) or solve numerical word problems.
Cued Explicit Recognition/Recall	A list of items (words, objects, textures, patterns, pictures, sounds) is presented and the subject is subsequently tested with cues to recall previously presented material.
Delayed Match to Sample	A stimulus that is followed by a probe item after a brief delay; subject is then asked to recall if the probe item was presented before the delay.
Emotion Induction	Stimuli with emotional valence (i.e. statements, films, music, pictures) to induce effect on mood.
Encoding	Memorize stimuli such as words, pictures, letters, etc. Incidental Encoding: A task in which the subject is creating new memories without purposely knowing that memorization is the task at hand. Their memories are created thorough working in their environment and picking up information in the process.
Face Monitor/Discrimination	View face passively or discriminate human faces according to their order, gender, location, emotion, or appearance, etc.
Film Viewing	View movies or film clips.
Finger Tapping/Button Press	Tap fingers or press a button in a cued/non-cued manner.
Go/No-Go	Perform a binary decision (go or no-go) on a continuous stream of stimuli.
n-back	Indicate when the current stimulus matches the one from n steps earlier in the sequence. Load factor n can be adjusted to make the task more or less difficult.
Orthographic Discrimination	View letters and discriminate according to some written/printed feature (i.e. uppercase/lowercase, alphabetic order, same/different spelling of words, vowel/consonant, font type/size).
Passive Listening	Listen to auditory stimuli (speech, noise, tones, etc.) and make no response.
Passive Viewing	View visual stimuli (objects, faces, letter strings, etc.) and make no response. If the presented stimuli are faces, the experiments are co-coded with Face Monitor/Discrimation. If presented stimuli are words, the experiments are not coded as passive viewing but rather as Reading (Covert).
Phonological Discrimination	View or listen to phonemes, syllables, or words and discriminate according to some feature of their sounds (rhyming, number of syllables, homophones, pronounceable nonwords, etc.).
Reading (Covert)	Silently read words, pseudo-words, characters, phrases, or sentences.
Reading (Overt)	Read aloud words, pseudo-words, logograms, phrases, or sentences.

Table S1 (cont.): Definitions of 26 BrainMap paradigm classes tagged to experiments activating the IFJ. Only paradigm classes tagged to at least 5 experiments were included. The definitions were extracted from BrainMap lexicon, available at http://www.brainmap.org/scribe/BrainMapLex.xls

Paradigm Class	Definition
Reading (Covert)	Silently read words, pseudo-words, characters, phrases, or sentences.
Reading (Overt)	Read aloud words, pseudo-words, logograms, phrases, or sentences.
Reward	A stimulus that serves the role of reinforcing a desired response.
Semantic Monitor/Discrimination	Discriminate between the meanings of individual lexical items or to indicate if target word is semantically related to the probe word.
Stroop-Color Word	Name the color of the ink for a list of words (color names) printed in congruent/incongruent colors, or determine if ink color and color name are congruent/incongruent. Color-congruent stimuli: ink color and color name are the same (e.g. the word "GREEN" printed in green ink). Color-incongruent stimuli: ink color and color name differ (e.g. the word "GREEN" printed in red ink).
Task Switching	Switch from one task or goal to another.
Tone Monitor/Discrimination	Listen to tones passively or discriminate according to a sound property (i.e. order, timing, pitch, frequency, amplitude), and/or detect presence/absence of a tone.
Visual Object Identification	Identify an object based on its visual attributes (e.g. shape, color, viewing angle), or detect/discriminate changes on the object's visual properties (e.g. size, illumination, position, relation between parts).
Visuospatial Attention	Make cued/ noncued shifts of visual attention to a particular spatial location in the visual field. Responses can be overt (with eye movement to target location) or covert (fixating on a central target while paying attention to spatial location changes of peripheral target).
Wisconsin Card Sorting Test	Sort cards into groups based on some dimension (i.e.: color, form, or number) that is changed intermittently, and requires subject to identify a new correct group dimension.
Word Generation (Covert)	Semantic: Listen to or view nouns and silently generate an associated verb, or view a category and silently generate as many exemplars as possible. Orthographic: Listen to or view a letter and silently generate as many words as possible that start with that letter. Phonologic: Listen to or view a word and silently generate words that rhyme.
Word Generation (Overt)	Semantic: Listen to or view nouns and overtly generate an associated verb, or view a category and overtly generate as many exemplars as possible. Orthographic: Listen to or view a letter and overtly generate as many words as possible that start with that letter. Phonologic: Listen to or view a word and overtly generate words that rhyme.

Table S2: Top 5 tasks with the highest probabilities of recruiting a co-activation pattern involving the IFJ

Co-activation Pattern C1	
Task	**Pr (C1 | Task)**
Phonological Monitor/ Discrimination	0.51
Semantic Monitor/ Discrimination	0.50
Covert Reading	0.45
Covert Word Generation	0.42
Face Monitor/ Discrimination	0.41

Co-activation Pattern C2	
Task	**Pr (C2 | Task)**
Task Switching	0.61
Counting/ Calculation	0.54
Wisconsin Card Sorting Task	0.47
Overt Reading	0.40
Cued Recognition/ Recall	0.39

Co-activation Pattern C3	
Task	**Pr (C3 | Task)**
Go/ No-Go	0.63
Stroop – Color Word	0.51
Reward	0.48
Delayed Match to Sample	0.47
Overt Reading	0.45

Table S3-A: Experiments with the highest probabilities of recruiting co-activation pattern C1 of IFJ

Phonological Discrimination					
PMID	**Author**	**Title**	**Exp**	**Contrast**	**Pr**
16168736	Tyler 2005	Temporal and frontal systems in speech comprehension: an fMRI study of past tense processing	2	Real regular verbs – real irregular verbs	0.92
11230098	Xu 2001	Conjoint and extended neural networks for the computation of speech codes: the neural basis of selective impairment in reading words and pseudowords	4	Real-word rhyming – color-matching with letters (Group)	0.89
11230098	Xu 2001	Conjoint and extended neural networks for the computation of speech codes: the neural basis of selective impairment in reading words and pseudowords	7	Alternate-case rhyming – color-matching with letters (Group)	0.80
Semantic Monitoring/ Discrimination					
PMID	**Author**	**Title**	**Exp**	**Contrast**	**Pr**
14644105	Poeppel 2004	Auditory lexical decision, categorical perception, and FM direction discrimination differentially engage left and right auditory cortex	5	Lexical decision of phonologically per missible targets vs. frequency-modulated signals	0.95
11502262	Wagner 2001	Recovering meaning: left prefrontal cortex guides controlled semantic retrieval	4	4 target items > 2 target items (strong cue-correct response association)	0.90
11502262	Wagner 2001	Recovering meaning: left prefrontal cortex guides controlled semantic retrieval	6	Weak > strong cue-correct responses association (2 target items)	0.89
Covert Reading					
PMID	**Author**	**Title**	**Exp**	**Contrast**	**Pr**
17110132	Jobard 2007	Impact of modality and linguistic complexity during reading and listening tasks	3	Conjunction of reading and listening irrespective of the linguistic complexity	0.75
19155745	Small 2009	Your brain on Google: patterns of cerebral activation during internet searching	2	Reading task in Internet-naïve group	0.71
19155745	Small 2009	Your brain on Google: patterns of cerebral activation during internet searching	3	Internet task in Internet-savvy group	0.70

Each row shows one of the top 3 experiments with the highest probabilities of recruiting co-activation pattern C1 of IFJ and recruiting one of the top 3 tasks with the highest probabilities of recruiting C1, namely "Phonological Discrimination", "Semantic Monitoring/ Discrimination", and "Covert Reading". The "PMID" and "Title" columns list the PubMed ID and title of each study respectively. The "Author" column lists the surname of the first author and the year of publication of each study. The "Exp" column lists the experiment's order in the respective study as reported in BrainMap. The "Contrast" column lists the experimental contrast of each experiment. The "Pr" column shows the probability that each experiment would recruit the co-activation pattern C1.

Table S3-B: Experiments with the highest probabilities of recruiting co-activation pattern C2 of IFJ

Task Switching					
PMID	**Author**	**Title**	**Exp**	**Contrast**	**Pr**
18971462	Xue 2008	Neural Substrates for Reversing Stimulus–Outcome and Stimulus–Response Associations	2	Full-reversal learning – No-reversal learning	0.75
12457760	Sylvester 2003	Switching attention and resolving interference: fMRI measures of executive functions	3	Counter-switching task (blocked design)	0.71
10401985	Omori 1999	Neuronal substrates participating in attentional set-shifting of rules for visually guided motor selection: a functional magnetic resonance imaging investigation	2	Conjunction among alternate vs. rest, tie vs. rest, win vs. rest, lose vs. rest	0.70

Task Switching					
PMID	**Author**	**Title**	**Exp**	**Contrast**	**Pr**
11162272	Zago 2001	Neural Correlates of Simple and Complex Mental Calculation	4	Compute vs. retrieve masked by compute vs. read	0.95
11162272	Zago 2001	Neural Correlates of Simple and Complex Mental Calculation	2	Compute vs. read	0.88
10931772	Pesenti 2000	Neuroanatomical substrates of arabic number processing, numerical comparison, and simple addition: a PET study	4	Addition vs. rest	0.84

Wisconsin Card Sorting Test					
PMID	**Author**	**Title**	**Exp**	**Contrast**	**Pr**
8524452	Berman 1995	Physiological activation of a cortical network during performance of the Wisconsin Card Sorting Test: A positron emission tomography study	1	Wisconsin Card Sorting Task > Control	0.61
12032364	Konishi 2002	Hemispheric asymmetry in human lateral prefrontal cortex during cognitive set shifting	2	Event B (omitting the negative feedback stimulus) – Event C (“null” change instruction)	0.59
12944506	Konishi 2003	Transient Activation of Superior Prefrontal Cortex during Inhibition of Cognitive Set	2	Inhibition – Control (Subjects aware of the dimensional changes)	0.52

Each row shows one of the top 3 experiments with the highest probabilities of recruiting co-activation pattern C2 of IFJ and recruiting one of the top 3 tasks with the highest probabilities of recruiting C2, namely “Task Switching”, “Counting/ Calculation”, and “Wisconsin Card Sorting Test”. The “PMID” and “Title” columns list the PubMed ID and title of each study respectively. The “Author” column lists the surname of the first author and the year of publication of each study. The “Exp” column lists the experiment’s order in the respective study as reported in BrainMap. The “Contrast” column lists the experimental contrast of each experiment. The “Pr” column shows the probability that each experiment would recruit the co-activation pattern C2.

Table S3-C: Experiments with the highest probabilities of recruiting co-activation pattern C3 of IFJ

Go/No-Go					
PMID	**Author**	**Title**	**Exp**	**Contrast**	**Pr**
20016103	Chikazoe 2009	Preparation to Inhibit a Response Complements Response Inhibition during Performance of a Stop-Signal Task	4	Disjunction analysis: Stop vs. Uncertain-go but not Uncertain-go vs. Certain-go	0.80
19718655	Simoes-Franklin 2010	Executive function and error detection: The effect of motivation on cingulate and ventral striatum activity	1	Go – No-go with punishment > Go – No-go without punishment	0.76
21903198	Zandbelt 2011	Reduced proactive inhibition in schizophrenia is related to corticostriatal dysfunction and poor working memory	14	Successful Stop > Go- with 0% stop-signal probability	0.76
Stroop – Color Word					
PMID	**Author**	**Title**	**Exp**	**Contrast**	**Pr**
21352930	Pompei 2011	Familial and disease specific abnormalities in the neural correlates of the Stroop Task in Bipolar Disorder	2	Interference – neutral (healthy controls group)	0.88
21352930	Pompei 2011	Familial and disease specific abnormalities in the neural correlates of the Stroop Task in Bipolar Disorder	3	Interference – neutral (healthy relatives of bipolar patients)	0.77
12738340	Weiss 2003	Brain activation patterns during a selective attention test-a functional MRI study in healthy volunteers and patients with schizophrenia	1	Modified Stroop task (healthy subjects manually responded to printed color of word)	0.60
Reward					
PMID	**Author**	**Title**	**Exp**	**Contrast**	**Pr**
18549791	Knutson 2008	Neural antecedents of the endowment effect	9	Activation for the period when subjects saw the prices	0.84
18549791	Knutson 2008	Neural antecedents of the endowment effect	7	Activation for the period when subjects saw the products	0.82
20399735	Peters 2010	Episodic Future Thinking Reduces Reward Delay Discounting through an Enhancement of Prefrontal-Mediotemporal Interactions	5	Positive correlation between neural tag effect (episodic > control) and behavioral tag effect (control > episodic)	0.76

Each row shows one of the top 3 experiments with the highest probabilities of recruiting co-activation pattern C3 of IFJ and recruiting one of the top 3 tasks with the highest probabilities of recruiting C1, namely "Go/No-Go", "Stroop – Color Word", and "Reward". The "PMID" and "Title" columns list the PubMed ID and title of each study respectively. The "Author" column lists the surname of the first author and the year of publication of each study. The "Exp" column lists the experiment's order in the respective study as reported in BrainMap. The "Contrast" column lists the experimental contrast of each experiment. The "Pr" column shows the probability that each experiment would recruit the co-activation pattern C3.

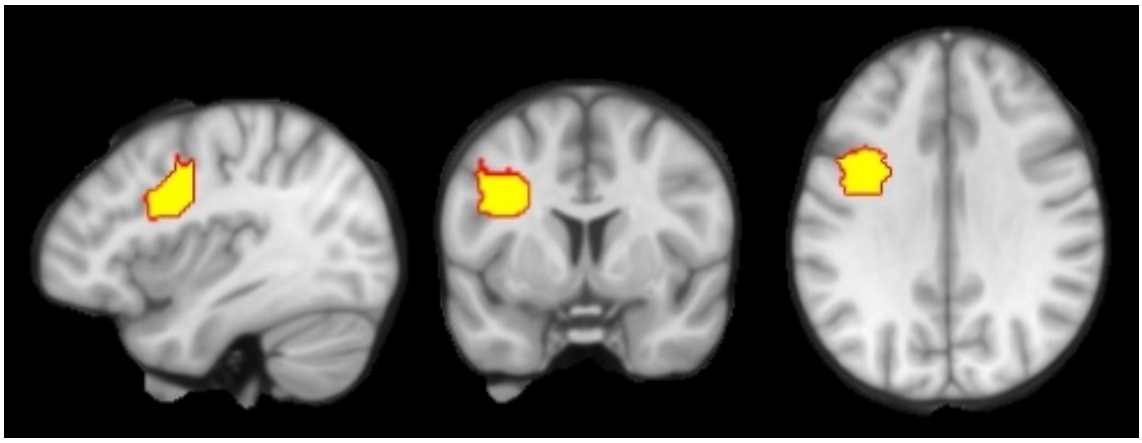

x = -37 y = 5 z = 31

Figure S1: Illustration of the IFJ (Muhle-Karbe et al., 2015) in the sagittal, coronal and transversal plane.

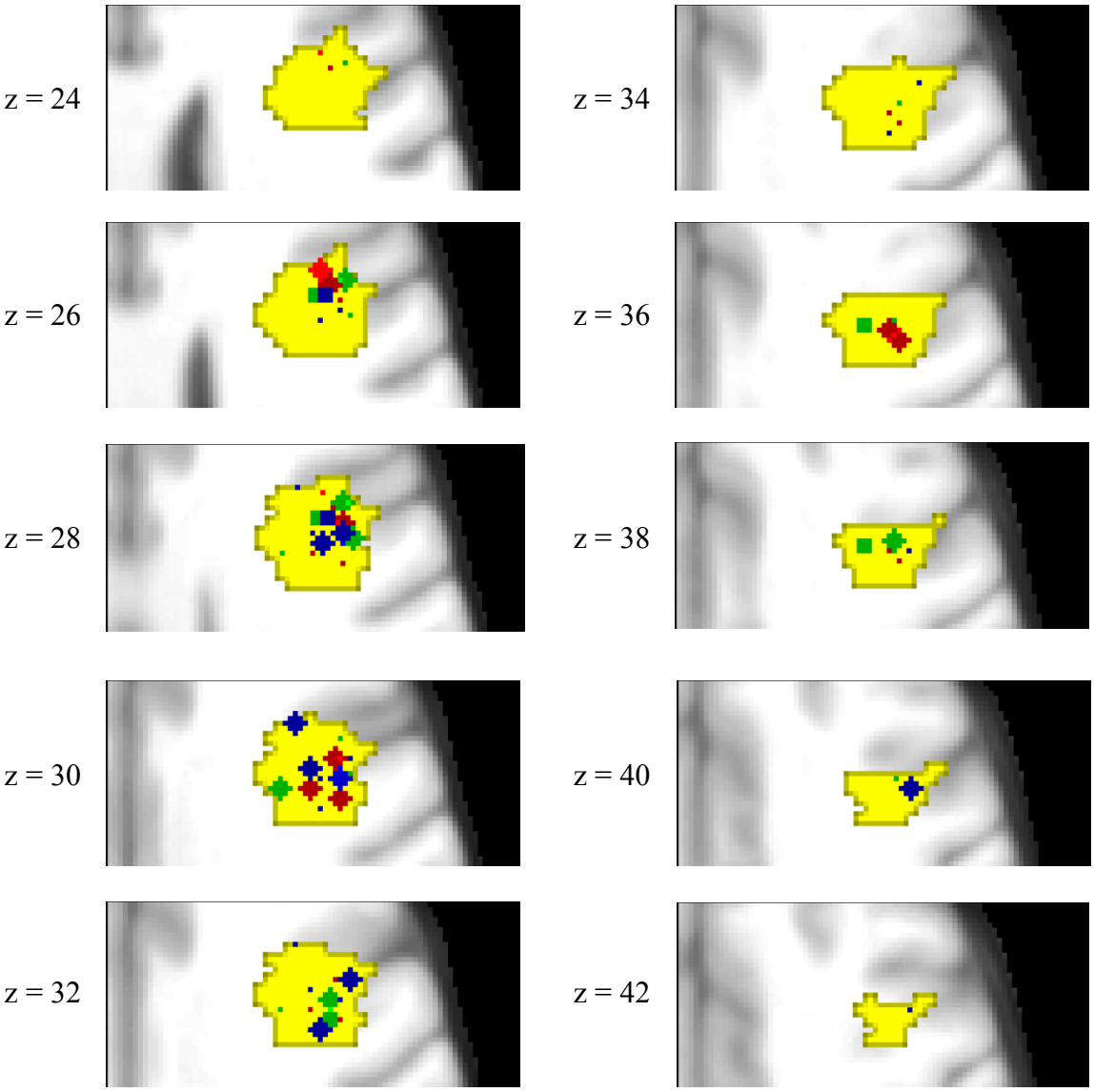

Figure S2: Volumetric slices suggesting the co-activation patterns overlap within the IFJ. The yellow areas delineate the IFJ. The colored dots correspond 2-mm-radius spheres centered about the activation foci reported by the top 3 experiments which have the highest probabilities of recruiting co-activation patterns of IFJ and recruit one of the top 3 tasks with the highest probabilities of recruiting the given co-activation pattern. Blue, red and green dots correspond to the activation foci associated with co-activation pattern C1, C2, and C3, respectively.